

TAXONOMIC COMMENTS OF A *GLOSSOTHERIUM* SPECIMEN FROM THE PLEISTOCENE OF CENTRAL CHILE

Hans P. Püschel (1), Thomas A. Püschel (2) and David Rubilar-Rogers (1)

(1) Área Paleontología, Museo Nacional de Historia Natural, Casilla 787, Santiago, Chile.

(2) School of Earth and Environmental Sciences, University of Manchester, Oxford Road, Manchester, M13 9PL, UK.

ABSTRACT

The Mylodontidae family was once one of the most diverse Pleistocene fauna in South America. Within this family, the genus *Glossotherium* showed a wide distribution in the southern cone with a single record in Chile SGO.PV.2 housed at the National Museum of Natural History of Chile. Provided that the species allocation of this individual as *Glossotherium lettsomi* was made 48 years ago, a revision was carried out considering new taxonomic studies. Based on this recent information, a new diagnosis of the specimen was carried out. Principal component analyses (PCA) and a linear discriminant analyses (LDA) were performed using comparative cranial data obtained from the literature in order to establish initial morphological affinities. In addition, a phylogenetic inference analysis was conducted to establish the phylogenetic position of SGO.PV.2. Finally, the first description of the post-cranial skeleton of SGO.PV.2 is also provided. The results of the different analyzes performed in this study indicate that SGO.PV.2 should be assigned to the species *Glossotherium robustum*, thus currently representing the only record of this species in Chile.

Key words: Xenarthra, Mylodontidae, Morphology, Upper Pleistocene, Chile

RESUMEN

Comentarios Taxonómicos de un espécimen de *Glossotherium* del Pleistoceno de Chile Central. La familia Mylodontidae fue una de las más diversas de la fauna del Pleistoceno en Sudamérica. Dentro de esta, el género *Glossotherium* poseía una amplia distribución en el cono sur, con un solo registro en Chile, SGO.PV.2 depositado en el Museo Nacional de Historia Natural de Chile. Dado que la asignación de especie de este ejemplar como *Glossotherium lettsomi* se realizó hace 48 años, se llevó a cabo una revisión de esta considerando nuevos estudios taxonómicos. Con estos nuevos antecedentes, se realizó una nueva diagnosis del ejemplar, análisis de componentes principales (PCA) y análisis discriminantes lineales (LDA) en los que se utilizaron datos craneales de estudios previos con ejemplares de *Glossotherium robustum*. Por otra parte, se realizó un análisis filogenético basado en estudios previos, considerando sólo caracteres craneodentales de SGO.PV.2 con el fin de establecer su relación con los integrantes del clado o familia. Por último, se realizó una descripción inédita del esqueleto postcraneal de SGO.PV.2. Los resultados del conjunto de análisis realizados indican la asignación de SGO.PV.2 a la especie *Glossotherium robustum*, siendo el único registro de esta especie en Chile.

Palabras Claves: Xenarthra, Mylodontidae, Morfología, Pleistoceno Superior, Chile

INTRODUCTION

One of the most documented groups within the superorder Xenarthra is pilosans. This group comprises two sub-orders, Vermilingua (*i.e.*, extant and extinct anteaters) and Folivora (*i.e.*, extant arboreal sloths, as well as extinct terrestrial sloths) (Delsuc *et al.* 2001). During the Quaternary in South America the sloth family Mylodontidae was one of the most diverse fauna within Folivora (Pitana *et al.* 2013). The genus *Glossotherium* was among the most common genera with records in the Chapadmalan-Lujaniano (Pliocene-Pleistocene) from different localities in Argentina, Bolivia, Brazil, Chile, Colombia, Ecuador, Paraguay, Peru and Uruguay (Cabrera 1936, Casamiquela 1968, Cartelle and Fonseca 1981, Figini *et al.* 1987, Esteban 1996, McAfee 2007, 2009). Based on morphological differences, it has been proposed that at least two different species existed during the South American Pleistocene. The first one would have been *Glossotherium robustum*, the southernmost species, distributed between 20° S and 40° S occupying Argentina, Brazil, Bolivia, Chile, Uruguay and Paraguay, while the second was *Glossotherium* sp., the equatorial species, restricted between 5° S and 15° S, with records currently limited to the northeastern

region of Brazil (Pitana *et al.* 2013). However, more evidence is needed to confirm this proposed new species in order to assign it a name. Throughout the Pleistocene in North America and linked to the Great American Biotic Interchange, there was a taxon closely related to *Glossotherium* known as *Paramylodon harlani* (McAfee 2009).

In Chile there is a single record of *Glossotherium* (SGO.PV.2) housed at the National Museum of Natural History of Chile. The story of the discovery of this specimen and its cranial description can be found in Casamiquela (1968). In that study neither did the author provide a description of the postcranial skeleton nor did he analyze the whole available material in order to provide an accurate classification of the specimen. Consequently, the main objectives of this paper are, firstly, to corroborate the diagnosis of the specimen in the light of new studies after almost 50 years of its discovery, and secondly, to provide the pending description of the postcranial skeleton of the individual.

Taxonomic comments about the specimen

Based on diagnostic characteristics and cranial measurement proposed in previous studies (Kraglievich L. 1922, Cabrera 1936, Hoffstetter 1949), Casamiquela (1968) identified the species as *Glossotherium lettsomi*. However, according to Casamiquela (1968) since the measurements obtained could be placed between those of *Glossotherium lettsomi* and *Glossotherium robustum*, he thought it was better to accept a monospecific classification of *Glossotherium sensu stricto*. A subsequent revision of the same specimen (Labarca 2015) suggested that it corresponded to an individual of *Glossotherium robustum*. Labarca (2015) based his classification on the age indicated for the remains (Upper Pleistocene: Casamiquela 1968) and by taking into account more recent taxonomic proposals (Esteban 1996, Carlini and Scillato-Yané 1999) that considered *G. lettsomi* as synonymous of *G. robustum*. In a study reassessing the cranial characters of *Glossotherium* and *Paramylodon*, McAfee (2009) proposed a revised diagnosis for *Glossotherium robustum* based on a principal component analysis (PCA) of cranio-mandibular measurements.

Type locality, Horizon and Age

The outcrop is positioned 23 km from Lonquimay town (Malleco) travelling on the international road CH-181 in direction to Pino Hachado border crossing point (Figure 1). The approximate georeferenced coordinates are: 38°31'33.23"S, 71°12'6.00"O (latitude: -38.5259, longitude: -71.2017). These coordinates were inferred from the site description of Casamiquela (1968). However, due his vague description it is better to consider a 500-meter radio from this point. According to Casamiquela (1968) the fossil comes from "formaciones periglaciales de vertiente" (slope periglacial formations), which belong to the Quaternary, probably Upper Pleistocene. Contrasting this description with the geological chart of the region (Suárez and Empanan 1997), the outcrop is located in Quaternary unconsolidated and undifferentiated sediments with pyroclastic intercalations. However, a geological fieldwork is still needed to precisely determine its exact location. The fossil age was determined by radiocarbon (¹⁴C) dating of individual amino acids of purified collagen with the use of XAD-2 resin in 10,960 ± 70 ¹⁴C years before present (CAMS#175740; Villavicencio 2016). After calibrating this age using the Calib 7.02 software (Stuiver and Reimer 1986-2014) and applying the calibration curve for the southern hemisphere SH13, the resulting age is 12,791 calibrated years before the present (range at 2σ 12,975-12,700 cal. years BP). This dating is consistent with the outcrop's estimated age. Taking into consideration that the last definition and dating of the GSSP (Global Stratotype Section and Point) for the base of the Holocene is 11,700 years b2 k (before AD 2000; Walker *et al.* 2008), it is possible to say that SGO.PV.2 lived in the Upper Pleistocene and near the Upper Pleistocene–Holocene boundary. That corresponds in the South American land mammal ages (SALMA) to the Lujanian (10,000-800,000 years ago; Flynn and Swischer 1995) near the upper boundary of this age.

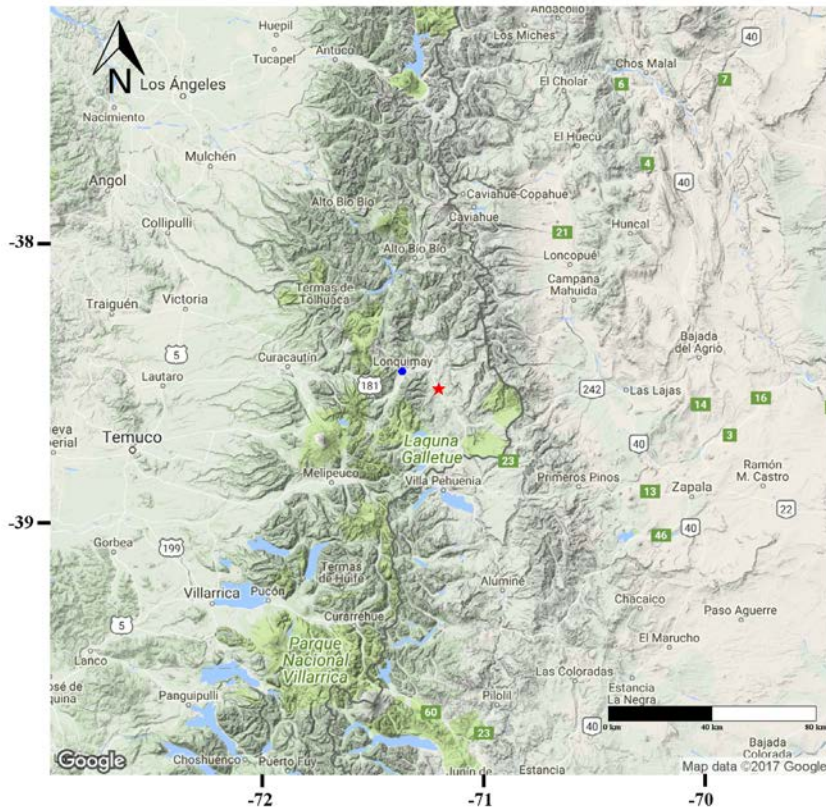


FIGURE 1. Region terrain map of the finding of SGO.PV.2; The main roads are indicated with their number and the cities are indicated by their name and a small white circle. The National Parks are indicated with green and the bodies of water with light blue. The thick gray line represents the frontier between Chile and Argentina. The red star indicates the SGO.PV.2 outcrop location, and the blue circle shows the Lonquimay town location. The geographic coordinates are in the margins in decimal degrees (DD). Map made with the ‘ggmap’ R package (Kahle and Wickham 2016)

MATERIAL AND METHODS

New diagnosis for the skull and species classification

The SGO.PV.2 *Glossotherium* specimen was studied in the vertebrate paleontological collections of the Museo Nacional de Historia Natural de Chile (MNHN). In the present paper, the diagnosis of McAfee (2009) was used to confirm that the remains corresponded to *Glossotherium robustum*. Cranial data from SGO.PV.2 was collected using a caliper while the comparative data from other individuals was extracted from previously published papers and used to carry out PCAs and linear discriminant analyses (LDAs) (see McAfee 2009, Pitana *et al.* 2013). When using the data from Pitana *et al.* (2013) to perform the LDA analysis, we calculated a correlation matrix to identify redundant variables. Maxillary width between M3 (WM3) was highly correlated with all other measurements, so this measurement was removed to reduce the number of variables. To estimate the missing values present in the McAfee (2009) data a multiple imputation procedure was performed using the R language (R Core Team, 2014) with the ‘mice’ package (van Buuren *et al.* 2015). The imputations obtained were averaged to obtain one dataset that was used in the further analyzes. Measurements were transformed using a Darroch and Mossiman (1985) approach to minimize size influence using scale-free ratios, which are dimensionless variables (Jungers *et al.* 1995). The PCAs were performed in PAST v. 3.11 (Hammer *et al.* 2008) using their respective correlation matrices to standardize the variables, thus avoiding possible problems when for instance a variable has a noticeably larger variance than others, which might increase its weight on the PCA. The R language (R Core Team, 2014) was used again to carry out the LDAs using the ‘Discriminer’ package (Sanchez 2013). In the first

LDA, the groups defined a priori were *Glossotherium robustum* and *Paramylodon harlani*. The obtained discriminant function was used to categorize SGO.PV.2 within one of these groups. The same procedure was repeated for the second LDA, although the groups defined a priori in this case were *Glossotherium robustum* and *Glossotherium* sp. In addition, we performed some phylogenetic inference analyses using Gaudin's (2004) dataset. This data matrix was used by including the morphological characters collected from SGO.PV.2 that were identifiable from a total of 201 cranio-dental traits (the SGO.PV.2 mandible traits were not considered). Subsequently, the same methodology applied by Gaudin (2004) was replicated using PAUP v. 4.0a147 (Swofford 2003) to obtain a single consensus tree.

Description of the postcranial skeleton of SGO.PV.2

As *Glossotherium robustum* was extensively described by Owen (1842), a rather brief description of each anatomical structure is given to emphasize differences and possible characters not previously described in the literature. All measurements were collected using a caliper, and all pictures were taken using a Nikon 5300 camera with an 18-55 mm lens. To describe the osteoderms we followed Hill (2006), by using the terms "superficial" and "deep" rather than "dorsal" and "ventral" to characterize more accurately these dermal elements.

RESULTS

New diagnosis of SGO.PV.2 based on McAfee (2009)

Systematic paleontology

Order Xenarthra Cope, 1889

Family Mylodontidae Gill, 1872

Genus *Glossotherium* Owen, 1840

species *Glossotherium robustum* Owen, 1842

Synonymy

Myiodon robustus Owen, 1842

Myiodon gracilis Burmeister, 1865

Pseudolestodon lettsomi Gervais and Ameghino, 1880

Pseudolestodon myloides Gervais and Ameghino, 1880

Pseudolestodon morenoii Gervais and Ameghino, 1880

Glossotherium wegneri Spillmann, 1931

(Figures 2, 6, 7, 8, 9, 10, 11, 12, 13, 14, 15, 16, 17, 18, 19 and 20)

Material— SGO.PV.2 (=P 67-V-10-1 original designation) is composed of a skull, mandible, nine osteoderms or dermal ossicles, eight bones of the anterior extremities (left ulna, left semilunar bone, left first metacarpal, first right metacarpal, third left metacarpal, third proximal phalanx, third medial phalanx and the first left distal phalanx), seven bones of the posterior extremities (left calcaneus, right talus, left cuboid, right cuboid, fifth left metatarsal, fourth right metatarsal, external cuneiform or third left cuneiform), four elements of the hyoid apparatus (right and left stylohyal, left epihial, basithyrohyal (V-shaped bone)), five rib fragments (left T1 rib, right T4 rib, left T3 rib, unidentified right and two left ribs), seven cervical vertebrae (C1, C2, C3, C4, C5, C6 and C7) and eight dorsal vertebrae (T1, T2, T3, T4, T5, T6, T7 and T8).

Cranium (Figure 2 A-C): dental formula is 5/5, with C1 present; M2 is triangular in section; M4 is bilobate with posterior lobe narrower than the anterior lobe, which is compressed in a anteroposterior axis; length of the molariform tooth row (110.6 mm) corresponds to less than 80 percent of total tooth row length (145 mm), representing 76.28%; palatine length posterior to M4 is less than 30 mm (22.5 mm); ratio of the palate length posterior to M4 versus total maxillary-palatine length (208 mm) is less than 0.15 (0.108); skull is roughly dome-shaped in lateral profile; posterior skull higher between the postorbital process than posteriorly; rostrum narrows posteriorly toward the lacrimals, then the skull widens toward the rear portion; nasal cavity width is greater (91.2 mm) than the height (58.3 mm); ratio of lacrimal (123.5 mm) to postorbital widths (160 mm) is less than 1:1 (0.772), with postorbital processes greatly expanded; pterygoid sinuses are markedly swollen medially and closely spaced; parasagittal crest is wide.

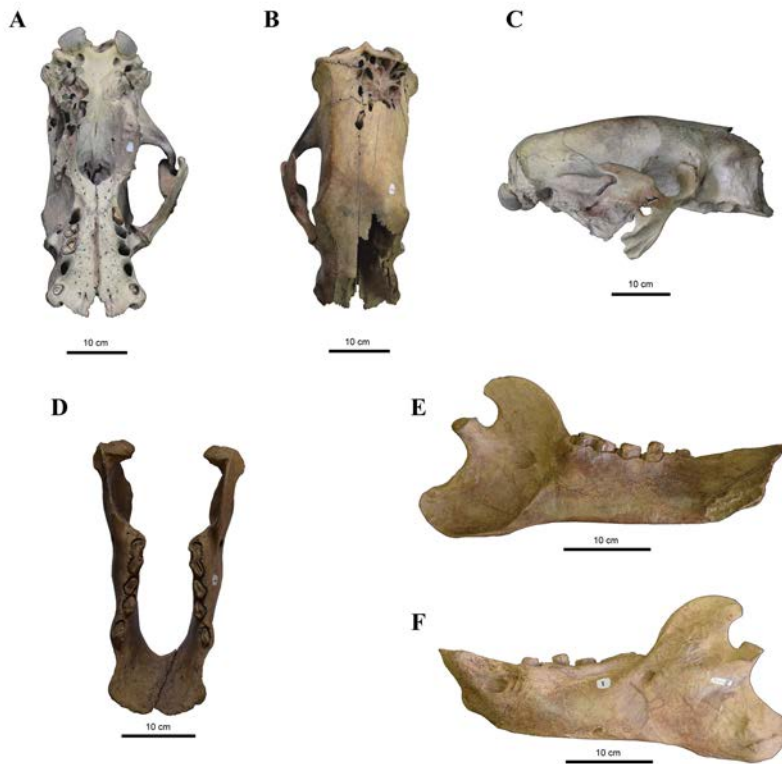


FIGURE 2. A-C SGO.PV.2 cranium; A, ventral view (anterior towards bottom); B, dorsal view (anterior towards bottom); C, right lateral view (anterior towards right, dorsal towards top); D-F SGO.PV.2 mandible; D, dorsal view (anterior towards bottom); E, left half of the mandible in medial view (anterior towards right, dorsal towards top); F, left half of the mandible in lateral view (anterior towards left, dorsal towards top)

Mandible (Figure 2 D-F): Although it was not considered by Casamiquela (1968), the SGO.PV.2 mandible was preserved. The condyle is lower in proportion to height of coronoid; anterior edge of coronoid process curved along upward slope; premental spout wide, with lateral flare at anterior margins creating a pronounced concavity along the lateral margins.

PCA and LDA results

The PCA plot of the first analysis incorporating SGO.PV.2 into the dataset obtained from McAfee (2007, 2009) shows a strong separation between *Glossotherium robustum* and *Paramylodon harlani* (Figure 3). The two 95% confidence interval ellipses do not overlap. SGO.PV. 2 was located within the *Glossotherium robustum* ellipse. Table 1 summarizes the PCA loadings. The anterior width (AntW), lacrimal width (LacW), and postorbital width (PorbW) had the highest scores in PC1. Total length (SKL), occipital condyle width (OcCndW), and lacrimal-squamosal length (LacSqL) registered the highest scores in PC2. The cross-validated confusion matrix obtained from the LDA using the same data showed that all the individuals were correctly classified in their respective species (Table 2). The SGO.PV.2 specimen was classified as *Glossotherium robustum* using the obtained discriminant function.

The second PCA incorporating SGO.PV.2 into Pitana's *et al.* (2013) dataset showed a separation between *Glossotherium robustum* and the two individuals classified as *Glossotherium* sp. (Figure 4: MCL 4027, 4303). In this case SGO.PV.2 was placed again within the *Glossotherium robustum* 95% confidence interval. Table 3 summarizes the PCA loadings. The maxilla width between M1 (WM1), maxilla width between M3 (WM3), and maxilla width between M4 (WM4) had the highest scores in PC1, whereas palate

TABLE 1. Cranial principal component (PCA) loadings. Higher loadings are in bold. Total length (SKL), anterior width (AntW), lacrimal width (LacW), postorbital width (PorbW), posterior width (PostW), anterior height (AntH), lacrimal height (LacH), postorbital height (PorbH), posterior height (PostH), occipital condyle width (OcCndW), maxillary-palate length (M-PL), lacrimal-squamosal length (LacSql), post-M4 length (postM4), molariform tooththrow length (M1-M4L), M1 length (M1L), M2 length (M2L), M3 length (M3L), M4 length (M4L)

	PC 1	PC 2
SKL	0.104	0.480
AntW	0.318	0.072
LacW	0.317	0.020
PorbW	0.244	0.078
PostW	0.133	-0.466
AntH	0.224	-0.305
LacH	0.267	-0.103
PorbH	-0.042	-0.179
PostH	0.239	0.346
OcCndW	-0.256	0.278
M-PL	-0.198	0.386
LacSql	-0.303	-0.001
postM4	-0.218	-0.029
M1-M4L	-0.248	-0.190
M1L	-0.232	-0.098
M2L	-0.197	-0.099
M3L	0.136	0.011
M4L		

TABLE 2. LDA confusion matrix. The classification formed a priori *Glossotherium robustum* and *Paramylodon harlani* (Original) was contrasted with the classification predicted after making LDA's cross-validation. In the last row the "classification" function was used in SGO.PV-2 indicated by ?, since it was not specified *a priori* its belonging to neither of the two groups

Original	Predicted	
	<i>Glossotherium robustum</i>	<i>Paramylodon harlani</i>
<i>Glossotherium robustum</i>	13	0
<i>Paramylodon harlani</i>	0	14
?	1	0

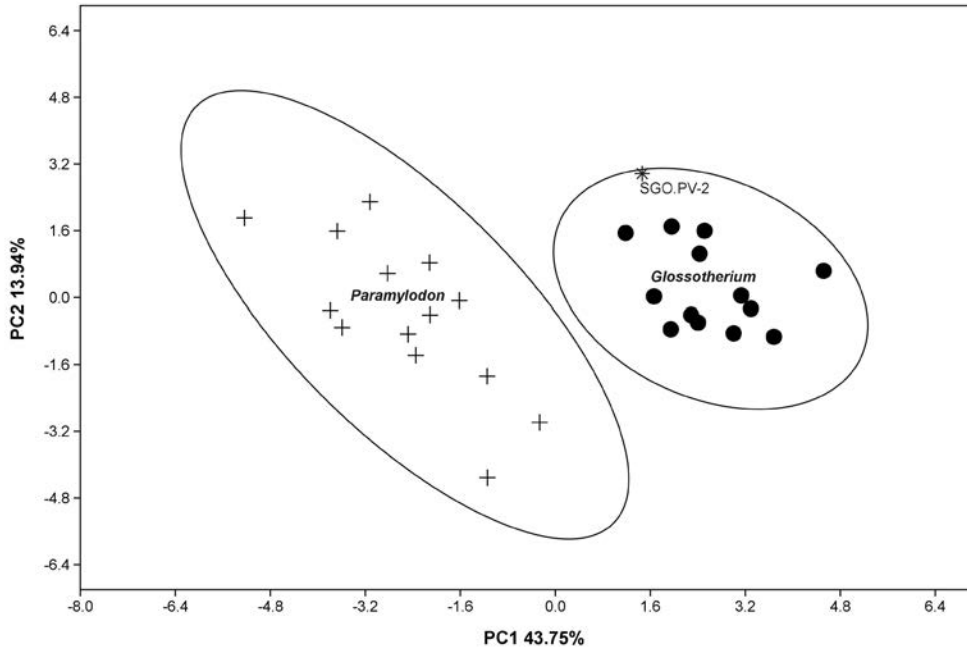


FIGURE 3. Principal component analysis (PCA) of cranial measurements; + correspond to *Paramylodon harlani* and • correspond to *Glossotherium robustum* (data obtained from McAfee 2007, 2009). SGO.PV.2 is indicated with *

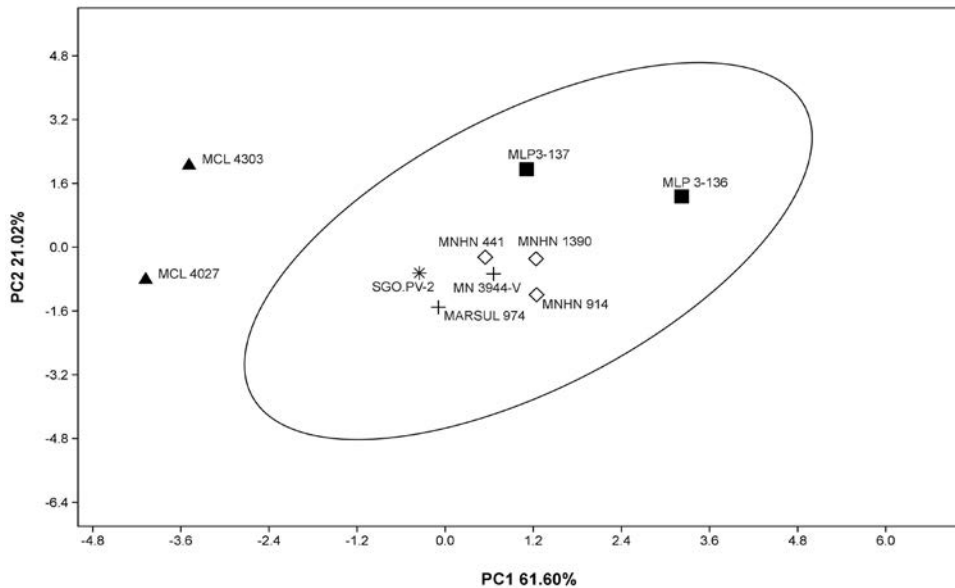


FIGURE 4. Principal component analysis (PCA) of cranial measurements; +, ■ y ◇ correspond to *Glossotherium robustum* (specimens from Argentina, Uruguay and southern Brasil); ▲ correspond to *Glossotherium* sp. (specimens from northeastern Brazil) (data obtained from Pitana *et al.* (2013)). SGO.PV.2 is indicated with *

TABLE 3. Cranial principal component (PCA) loadings. Higher loadings are in bold. Palate length (LP), upper dental row length (LUDR), maxilla width between M1 (WM1), maxilla width between M2 (WM2), maxilla width between M3 (WM3), maxilla width between M4 (WM4), maxilla width between M5 (WM5) and zygomatic arch width (WZA)

	PC 1	PC 2
LP	-0.435	0.133
LUDR	-0.443	0.012
WM1	0.432	-0.131
WM2	0.158	-0.517
WM3	0.423	-0.001
WM4	0.367	0.393
WM5	0.193	0.667
WZA	0.227	-0.313

TABLE 4. LDA confusion matrix. The classification formed *a priori* *Glossotherium robustum* and *Glossotherium* sp. (Original) was contrasted with the classification predicted after making LDA's cross-validation. In the last row the "classification" function was used in SGO.PV-2 indicated by ?, since it was not specified *a priori* its belonging to neither of the two groups

Original	Predicted	
	<i>G. robustum</i>	<i>Glossotherium</i> sp.
<i>G. robustum</i>	7	0
<i>Glossotherium</i> sp.	0	2
?	1	0

length (LP), maxilla width between M4 (WM4), and maxilla width between M5 (WM5) had the highest scores in PC2. The cross-validated confusion matrix obtained from the LDA using this dataset also showed that all the individuals were correctly classified (Table 4) and that SGO.PV. 2 was again classified as *Glossotherium robustum* using the obtained discriminant function.

Position of SGO.PV. 2 in the phylogeny of the suborder Folivora (Delsuc *et al.* 2001) (previously known as Tardigrada).

SGO.PV.2 was located in the obtained consensus tree within the Mylodontidae family (Figure 5) next to *Glossotherium*, thus supporting the results described above.

Description of post-cranial skeleton

Osteoderms

Within Mammalia, an interesting and unique feature that have some Xenarthra is the presence of osteoderms or dermal ossicles. These represent dermal ossifications within the integument. Within Pilosa, osteoderms are present in different extinct mylodontid ground sloths such as *Paramylodon* (*e.g.*, Sinclair 1910, Allen 1913, Stock 1925), *Myiodon* (*e.g.*, Moreno and Woodward 1899, Haro 2016, Martin 2016) and *Glossotherium* (*e.g.*, Hill 2006). By contrast with the highly derived osteoderms of glyptodonts, pampatheres, and armadillos which present complex articulations and surface ornamentation, the extinct mylodontid sloths possessed simple and isolated osteoderms, the presence of which is likely plesiomorphic for Xenarthra (Hill 2006). The mylodontoid osteoderms isolated nature was first described by Moreno and Woodward (1899) for *Neomyiodon* (= *Myiodon*; McKenna and Bell 1997), observing the osteoderms preserved in their life positions, free and isolated within the skin (Hill 2006). More recently, Haro (2016) described many osteoderms over the palmar surface of scaphoid, lunar, pisiform, hamate, and metacarpal of the manus of *Myiodon darwini* prior to cleaning and disarticulation. Associated with the SGO.PV.2 remains, a small box containing nine osteoderms was found. There was a small note indicating that they belonged to *Glossotherium*, but there was no SGO.PV.2 label. However, considering the color and texture of the sediment still attached to the osteoderms, the preservation color of the elements, and the features that they have; all seems to indicate that these elements are from the same specimen SGO.PV.2. The osteoderms are small, round or ovoid in shape, some more circular and others more elongated. They have between 13.8 mm and 21.5 mm in length, and between 7.7 mm and 14.3 mm. in width (Figure 6). As described for the late Pliocene species *Glossotherium chapadmalense* (Hill 2006), the superficial surface of each osteoderm in SGO.PV.2 is typically rough and irregularly pitted (Figure 6 A), whereas the deep surface is smooth and strongly convex (Figure 6 B). These elements are, at least in general terms, very similar to the other members of the Mylodontidae family during the Pleistocene. The same general description was used for *Myiodon darwini* (Haro 2016) and *Paramylodon harlani* (Merriam 1906, Sinclair 1910, Allen 1913). However, the bigger osteoderm sizes have been described for *Paramylodon*.

I) Axial skeleton

Hyoid apparatus

The mammalian hyoid apparatus has normally ten bony elements and two associated cartilages (tympanohyal and chondrohyal). From these anatomical elements, there are four pairs of bones (stylohyals, epihyals, ceratohyals, and thyrohyals) and an unpaired bone in adults, the basyhyal since it is formed by the fusion of the two primitive basihyals (Pérez *et al.* 2010). This configuration in Xenarthra changes dramatically because in this taxon there is a fusion of thyrohyals and basihyals to form a basithyrohyal (V-shaped bone) (Leidy 1855, Allen 1913, Pérez *et al.* 2000, Pérez *et al.* 2010). This is a trait very distinctive of the group (Figure 7 A).

From the previously described bones only four bony elements were preserved in this specimen: the right stylohyal (with some damage in the articular surface with the epihyal), the left stylohyal, the left epihyal and the basithyrohyal (Figure 7 B). The length of the left stylohyal in SGO.PV.2 is slightly larger than the total length of the stylohyal of *G. robustum* in Tambuso *et al.* (2015, figure 5) and Pérez *et al.* (2010, figure 6), both having the same measurements (Table 5). When comparing the value of the measurement

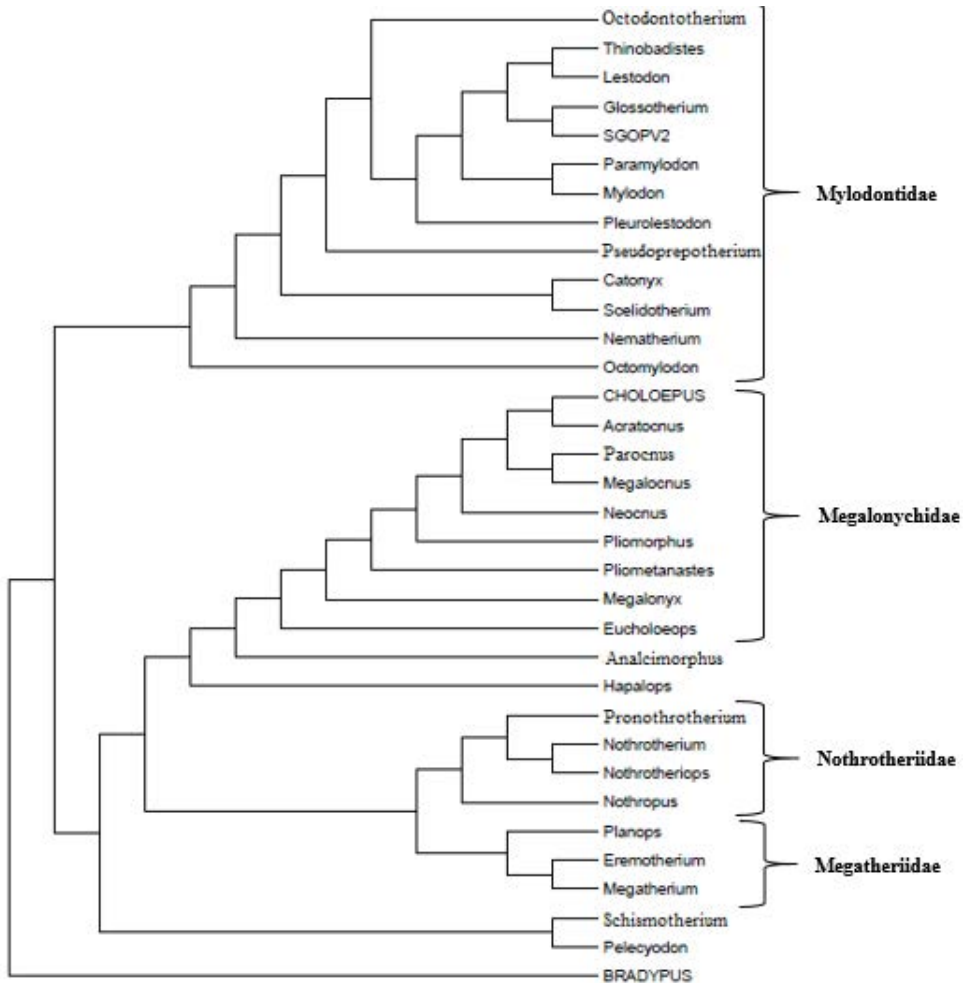


FIGURE 5. Phylogeny of suborder Folivora (equivalent to Tardigrada) including SGO.PV.2 performed in PAUP; this tree represents a strict consensus tree of all trees obtained according to the methodology described by Gaudin (2004) and using 201 craniodental characters. The families belonging to different genera are observed to the right in bold letters. Note the position of SGO.PV.2 within the family Mylodontidae next to *Glossotherium*

obtained from SGO.PV.2 with that of *Paramylodon*, it is possible to observe that *Paramylodon*'s stylohyal is slightly larger. The posterior end has muscle attachments for the stylohyoideus and occipitohyoideus muscles where the muscular angle is well developed being flat and lobed, while the anterior end has an articular surface that articulates with the epihyal highly developed with a convex face like in *Paramylodon* (Pérez *et al.* 2010). The right stylohyal is a mirror image of the other except for the damage of the articular surface for the epihyal. Otherwise, SGO.PV.2 left epihyal is very similar to the *Glossotherium robustum* specimen from Pérez *et al.* (2010), but considerably smaller than *Paramylodon* (Table 5). Finally, the SGO.PV.2 basithyrohyal has a V-shape typical of Xenarthra, being very similar and slightly larger than the *Glossotherium robustum* specimen from Pérez *et al.* (2010). However, even though its measurements are not extremely different when compared to those of *Paramylodon*, the greatest distance between thyrohyals in this element is considerably larger in *Paramylodon* (Table 5). In conclusion, all these elements are consistent with previous descriptions of the hyoid apparatus of *Glossotherium robustum* (Pérez *et al.* 2010).

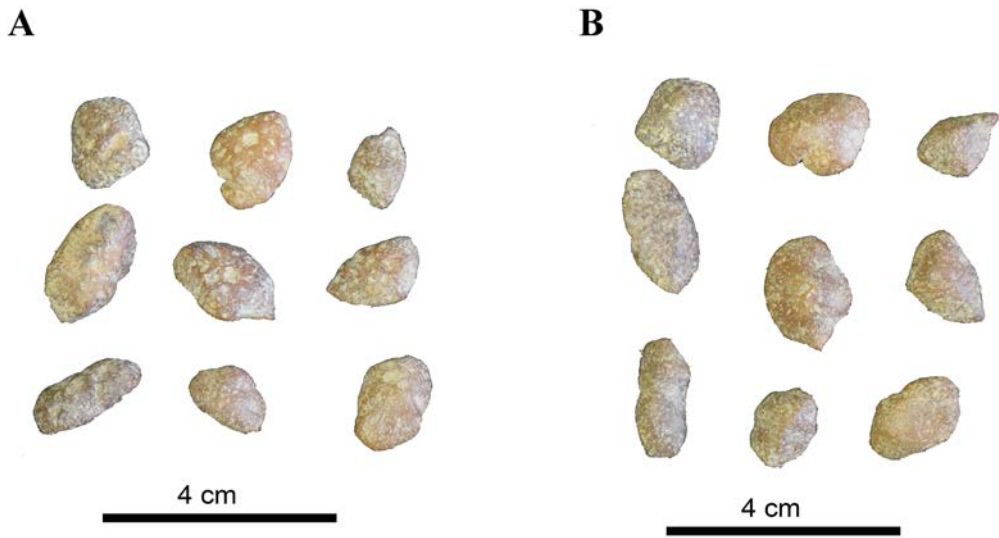


FIGURA 6. SGO.PV.2 osteoderms; A, superficial view; B, deep view

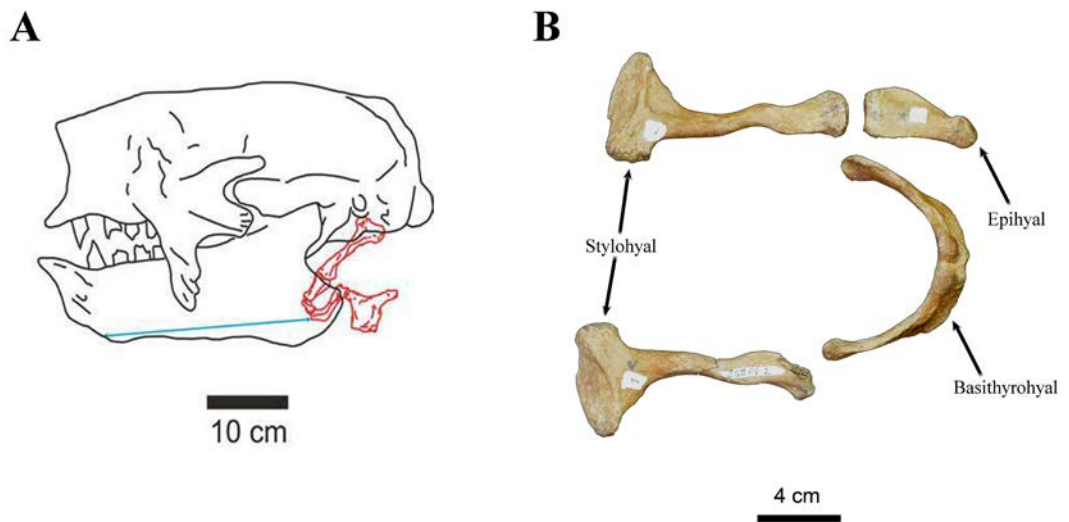


FIGURE 7. Hyoid apparatus of SGO.PV.2; A, skull and jaw of *G. robustum* and the hyoid apparatus of this species marked in red in left lateral view (extracted from Pérez *et al.* 2010); B, the hyoid apparatus bones preserved in SGO. PV-2, from left to right: the right stylohyal (with damage in the processes that articulates with the epihyal), left stylohyal, left epihyal and basithyrohyal (V-shaped bone)

TABLE 5. Measurements of elements of the hyoid apparatus of SGO.PV.2, along with comparisons to specimens of *Myiodon darwini* and *Paramyiodon harlani*. All measurements in millimeters and measured at its midpoint whenever were distances between cavities

	SGO.PV.2 (<i>Glossotherium robustum</i>)	<i>Glossotherium robustum</i> (From Pérez <i>et al.</i> 2010)	<i>Paramyiodon harlani</i> (From Pérez <i>et al.</i> 2010)
Hyoid apparatus			
Greatest length stylohyal	127.3	125.0	129.0
Stylohyal greatest posterior width	57.0	-	-
Stylohyal greatest anterior width	25.5	-	-
Stylohyal thinnest region	10.4	-	-
Greatest length epihyal	62.4	61.0	71.0
Width of the articular end for stylohyal	22.4	-	-
Width of the articular end for ceratohyal	11.3	-	-
Greatest distance between thyrohyals (Basithyrohyal)	80.7	75.0	109.0
Greatest length basihyal + thyrohyal (Basithyrohyal)	80.1	77.0	80.0
External width between ceratofacets (Basithyrohyal)	31.4	29.0	38.0
Internal width between ceratofacets (Basithyrohyal)	6.7	7.0	-

Vertebrae

It has been described (see Owen 1842) that *Glossotherium robustum* has seven cervical, sixteen dorsal and three lumbar vertebrae of which only the first twenty-two, counting from the first cervical to the dorsal vertebra, have mobility between them. The last dorsal and all lumbar vertebrae are fused to form a long sacrum. Of the total twenty-six vertebrae, only seven cervical and the first eight dorsal vertebrae were preserved in SGO.PV.2 (Figure 8).

a) Cervical vertebrae

The first cervical vertebra corresponds to the atlas (Figure 9) and its appearance fits the atlas described by Owen (1842: Plate VII) with a transversely oblong and broad shape surpassing even the skull. Posteriorly, the articular facets for the axis are rather circular and without a medial protrusion, which is characteristic of *Glossotherium* (Figure 9 B) in contrast to *Myiodon*, which presents ovate articular facets. In *Paramyiodon* this feature is variable (McAfee 2016). There is an indentation or notch between the anterolateral margin of the articular facets and the anteromedial beginning of the transverse processes, which is characteristic of *Glossotherium* and *Paramyiodon* by contrast to *Myiodon* (McAfee 2016). This feature is related to the orifices of the arterial canal. However, it is in the dorsal or superior orifices of the arterial canal that a difference can be observed with the previous description which mentions two more orifices, one anterior and one posterior (Owen 1842), resulting in a total of four orifices rather than the observed two that are seen in this specimen (Figure 9 C). One possible explanation for the difference in the number of dorsal

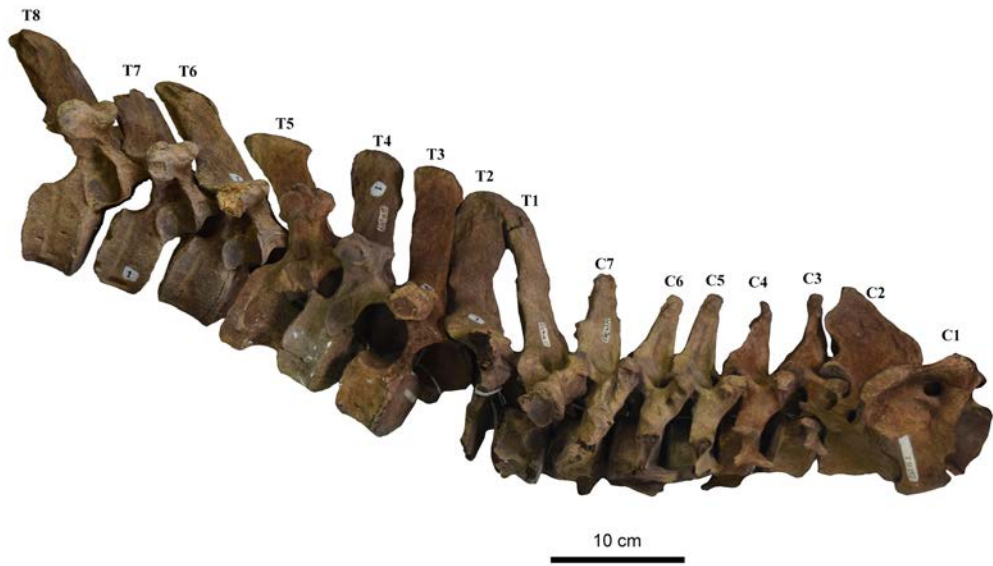


FIGURE 8. SGO.PV-2 vertebrae in right lateral view; From the total of twenty vertebrae, in this exemplary only eight cervical vertebrae and the first five dorsal vertebrae were preserved. Note the fusion of the spinous processes T1 and T2 and the absence of post-costal articular surfaces in dorsal vertebrae

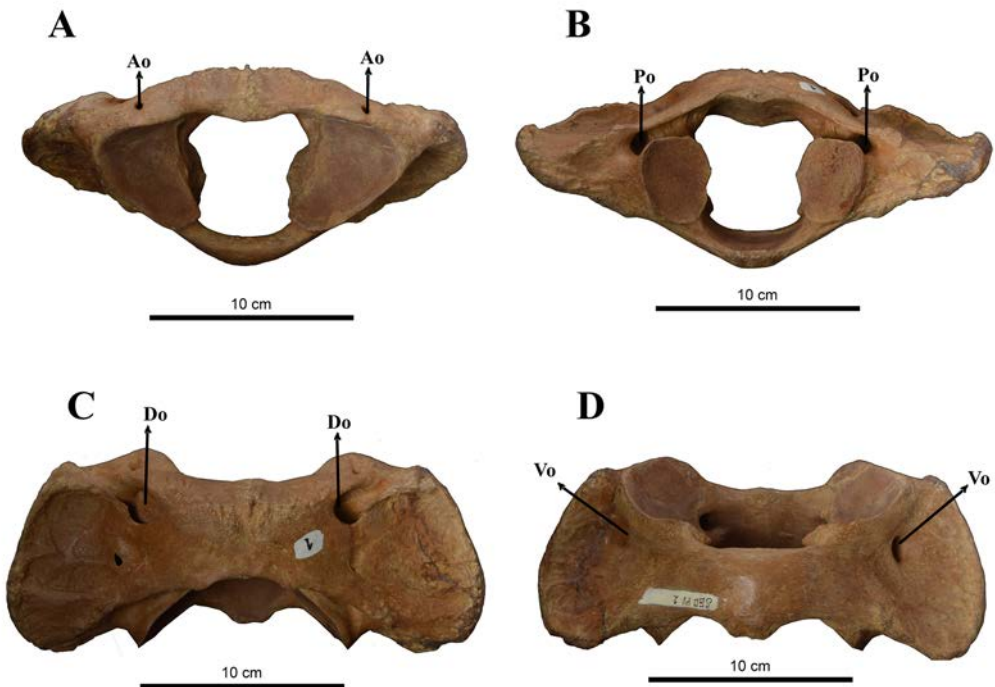


FIGURE 9. SGO.PV.2 atlas. A, anterior view; B, posterior view; C, dorsal view; D, ventral view. In C note two superior orifices of the vertebral canal, and a small postmortem fracture that looks like another vertebral canal orifice under the left one. Abbreviations: Ao, anterior vertebral orifice; Po, posterior vertebral orifice; Do, dorsal vertebral orifice; Vo, ventral vertebral orifice

orifices is that as it is observed in two very small foramina in the posterior margins of the dorsal surface in *Myiodon* and *Paramyiodon* (Allen 1913, Stock 1925, McAfee 2016), these differences could be the result of intraspecific variation. Another possible explanation for this divergence regarding the number of dorsal orifices could flow from the fact that Owen carried out a reconstruction of the surface of the atlas because the specimen he analyzed was damaged in that region. In fact, just before the description of these orifices he mentions the following: “In another atlas mutilated ...” “... apparently not of the same species of *Myiodon*” (Owen 1842). Hence, it seems likely that Owen used another mutilated atlas of a *Myiodon* to describe what was missing in his *Glossotherium* specimen. Consequently, there could be only two dorsal orifices of the arterial canal that correspond to the two anterior dorsal orifices of Owen (1842). The posterior dorsal orifices mentioned by Owen would be only part of the arterial canal that leads to the dorsal orifices in the specimen here described, being covered by a bony surface.

The two ventral orifices of the arterial canal (Figure 9 D) are small and more laterally and anteriorly situated than those of *Myiodon* and *Paramyiodon*. Both these genera present on each side of the ventral surfaces of the wings two large and connected openings near the middle where the body and wings meet (McAfee 2016). The size of the atlas is very similar in these three genera, although the anteroposterior wing length in SGO.PV.2 is considerably larger than in *Paramyiodon* and *Myiodon* (Table 6).

TABLE 6. Measurements of elements of the axial skeleton of SGO.PV.2, along with comparisons to specimens of *Myiodon darwinii* and *Paramyiodon harlani*. All measurements in millimeters and measured at its midpoint whenever were distances between cavities

	SGO.PV.2 (<i>Glossotherium robustum</i>)	<i>Paramyiodon harlani</i> (From Stock 1925, McAfee 2016)	<i>Myiodon darwinii</i> (From McAfee 2016)
Atlas		N=15	
Width between transverse processes	226.7	224.6 ± 9.2	223.9
Anteroposterior length of body	42.0	38.5 ± 3.5	29.3
Anteroposterior length of neural arch	59.2	50.2 ± 3.5	43.7
Width across posterior condyles (lateral edge to lateral edge)	99.8	97.4 ± 3.5	87.8
Width across anterior condyles	136.0	129.7 ± 5.0	141.3
Width between dorsal orifices of the arterial canal	82.1	86.6 ± 7.1	83.9
Anteroposterior wing length	94.2	79.2 ± 4.7	72.2
Width between anterior condyles	68.3	55.1 ± 5.1	60.4
Width between posterior condyles	46.0	-	-
Width between ventral orifices of the arterial canal	134.1	-	-
Width between posterior entries of the vertebralarterial canal	91.7	-	-
Axis		N=6	
Width between the odontoid process and the anterior articular processes	10.5	-	-
Width between anterior articular processes	46.7	-	-
Dorsoventral spinous process length	80.1	-	-
Greatest length along medial line of ventral surface	97.9	86.9 ± 3.5	-

(Table 6. Continuation)

	SGO.PV.2 (<i>Glossotherium</i> <i>robustum</i>)	<i>Paramylodon harlani</i> (From Stock 1925, McAfee 2016)	<i>Myiodon darwini</i> (From McAfee 2016)
Greatest height (dorsoventral)	161.2	139.6 ± 3.1	-
Greatest width between the posterior ends of transverse processes	123.9	154.0 ± 8.8	-
Dorsoventral diameter of centrum across posterior surface	50.1	47.7 ± 2.2	-
Greatest width of centrum	55.1	58.7 ± 3.5	-
Greatest transverse diameter of neural canal at anterior end	52.7	50.0 ± 5.9	-
Width across posterior zygapophysis	75.8	86.8 ± 7.8	-
Greatest width across lateral ends of anterior articular processes	98.0	98.1 ± 6.3	-
Distance from anterior border of lateral facet for atlas to posterior end of transverse process	93.5	99.0 ± 8.5	-
Cervical vertebra three (C3)			
Anteroposterior length of body	39.6	38.0	-
Width across centrum measured over the anterior face and between inner borders of vertebral arterial canals	61.2	75.3	-
Dorsoventral anterior body width	46.3	50.3	-
Dorsoventral length from ventral border of posterior face of centrum to tip of the spinous process	155.4	136.5	-
Greatest width across transverse processes	147.8	166.0	-
Cervical vertebra four (C4)			
Anteroposterior length of body	33.8	37.5	-
Width across centrum measured over the anterior face and between inner borders of vertebral arterial canals	67.5	76.7	-
Dorsoventral anterior body width	47.6	51.1	-
Dorsoventral length from ventral border of posterior face of centrum to tip of the spinous process	148.0	138.0	-
Greatest width across transverse processes	156.4	175.6	-
Cervical vertebra five (C5)			
Anteroposterior length of body	36.3	37.0	-
Width across centrum measured over the anterior face and between inner borders of vertebral arterial canals	66.2	77.2	-
Dorsoventral anterior body width	47.8	49.5	-

(Table 6. Continuation)

	SGO.PV.2 (<i>Glossotherium robustum</i>)	<i>Paramylodon harlani</i> (From Stock 1925, McAfee 2016)	<i>Mylodon darwinii</i> (From McAfee 2016)
Dorsoventral length from ventral border of posterior face of centrum to tip of the spinous process	156.4	-	-
Greatest width across transverse processes (the left process has a small fracture)	152.0	183.0	-
Cervical vertebra six (C6)			
Anteroposterior length of body	39.0	37.0	-
Width across centrum measured over the anterior face and between inner borders of vertebral arterial canals	69.0	77.2	-
Dorsoventral anterior body width	49.8	49.5	-
Dorsoventral length from ventral border of posterior face of centrum to tip of the spinous process	158.0	-	-
Greatest width across transverse processes (the right process has a fracture)	161.9	194.5	-
Cervical vertebra seven (C7)			
Anteroposterior length of body (the anterior side of the body has some erosion)	35.3	42.2	-
Width across centrum measured over the anterior face	65.1	94.2	-
Dorsoventral anterior body width	47.7	46.2	-
Dorsoventral length from ventral border of posterior face of centrum to tip of the spinous process	170.4	-	-
Greatest width across transverse processes	183.9	202.0	-
Dorsal vertebra one (T1)			
Anteroposterior length of body	42.3	46.7	-
Greatest width across centrum measured over the anterior face	60.3	62.8	-
Dorsoventral anterior body width	47.7	48.9	-
Dorsoventral length from ventral border of posterior face of centrum to tip of the spinous process (its great length is partially due the fusion with the spinous process of T2)	231.8	218.2	-
Greatest width across transverse processes	187.7	195.0	-
Dorsal vertebra two (T2)			
Anteroposterior length of body (all the posterior part of the body is missing)	7.1	52.2	-
Greatest width across centrum measured over the anterior face	59.0	60.2	-

(Table 6. Continuation)

	SGO.PV.2 (<i>Glossotherium</i> <i>robustum</i>)	<i>Paramylodon harlani</i> (From Stock 1925, McAfee 2016)	<i>Myiodon darwini</i> (From McAfee 2016)
Dorsoventral anterior body width	44.5	48.9	-
Dorsoventral length from ventral border of posterior face of centrum to tip of the spinous process	233.0	223.0	-
Greatest width across transverse processes (the right process has a small fracture)	167.7	173.2	-
Dorsal vertebra three (T3)			
Anteroposterior length of body (the posterior side of the body has some erosion)	49.5	55.0	-
Greatest width across centrum measured over the anterior face	58.8	66.7	-
Dorsoventral anterior body width	54.6	52.3	-
Dorsoventral length from ventral border of posterior face of centrum to tip of the spinous process	228.4	210	-
Greatest width across transverse processes	162.0	177.2	-
Dorsal vertebra four (T4)			
Anteroposterior length of body (the posterior side of the body has some erosion)	42.2	54.5	-
Greatest width across centrum measured over the anterior face	56.1	66.0	-
Dorsoventral anterior body width	55.6	56.2	-
Dorsoventral length from ventral border of posterior face of centrum to tip of the spinous process	221.3	193.0	-
Greatest width across transverse processes	157.6	174.0	-
Dorsal vertebra five (T5)			
Anteroposterior length of body (the posterior side of the body has some erosion and it has a great fracture in the anterior area of the body)	46.0	55.0	-
Greatest width across centrum measured over the anterior face (it has a great fracture in the anterior area of the body)	-	67.6	-
Dorsoventral anterior body width (it has a great fracture in the anterior area of the body)	-	59.0	-
Dorsoventral length from ventral border of posterior face of centrum to tip of the spinous process	211.1	192.0	-
Greatest width across transverse processes	148.3	176.0	-

(Table 6. Continuation)

	SGO.PV.2 (<i>Glossotherium robustum</i>)	<i>Paramylodon harlani</i> (From Stock 1925, McAfee 2016)	<i>Mylodon darwini</i> (From McAfee 2016)
Dorsal vertebra six (T6)			
Anteroposterior length of body (the posterior side of the body has some erosion)	52.7	57.0	-
Greatest width across centrum measured over the anterior face	59.5	70.6	-
Dorsoventral anterior body width	59.1	58.6	-
Dorsoventral length from ventral border of posterior face of centrum to tip of the spinous process	196.5	191.0	-
Greatest width across transverse processes	153.3	183.3	-
Dorsal vertebra seven (T7)			
Anteroposterior length of body (the posterior side of the body has some erosion)	47.7	59.0	-
Greatest width across centrum measured over the anterior face	57.3	72.5	-
Dorsoventral anterior body width	57.1	58.9	-
Dorsoventral length from ventral border of posterior face of centrum to tip of the spinous process (it has a great fracture in the top of the spinous process)	164.1	185.2	-
Greatest width across transverse processes	161.3	187.2	-
Dorsal vertebra eight (T8)			
Anteroposterior length of body (the posterior side of the body has some erosion)	52.4	62.0	-
Greatest width across centrum measured over the anterior face	62.5	75.3	-
Dorsoventral anterior body width	61.0	59.4	-
Dorsoventral length from ventral border of posterior face of centrum to tip of the spinous process	211.3	-	-
Greatest width across transverse processes	175.2	190.4	-

The second cervical vertebra corresponds to the axis (Figure 10) and its appearance is consistent with previous descriptions possessing a long body, posteriorly terminated by a vertical articular surface almost flat which articulates with the third cervical vertebra. Then it extends anteriorly forming a thick odontoid process, which it is truncated obliquely to form an articular surface that connects with the body of the atlas (Owen 1842). Measurements of this element in SGO.PV.2 are fairly similar to those of *Paramylodon* (Table 6). However, the former is notably higher and narrower than the latter.

A couple of differences were observed in SGO.PV.2 with respect to the drawing of Owen (1842: Plate VII). Firstly, in the odontoid process it is drawn and mentioned that the articular surface rests ventrally in the atlas (Figure 10 B-C). However, in this specimen there is also an apparent articular surface on the opposite side (i.e. on the dorsal side). This apparent articular surface would not be such and it would be related to the movement and contact with the transverse ligament that helps to hold the odontoid in place and make it a pivot joint. This feature is also shared with *Paramylodon* (McAfee personal communication). It is possible that in the specimen analyzed by Owen this feature was not as noticeable as in the *Glossotherium* analyzed here, which could explain this omission in his drawings. Secondly, in this drawing only two tubercles are observed on each transverse process, while in the analyzed specimen it is possible to see only one of considerable size and a small bump where the other one should be (Figure 10 B). This could be due to intraspecific variation in the transverse processes within this species.

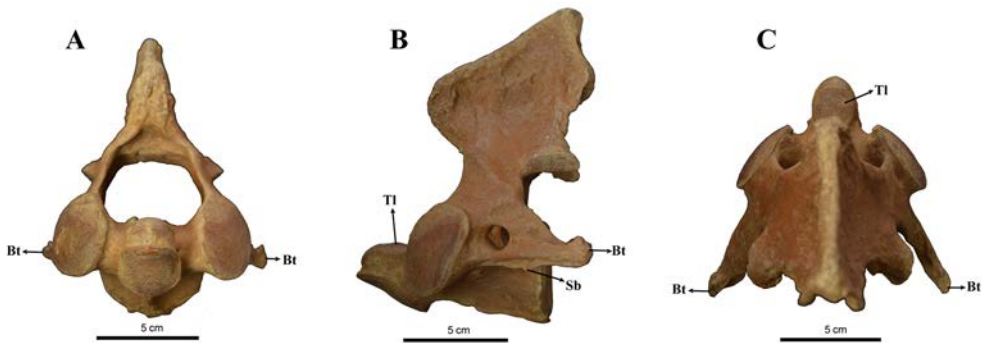


FIGURE 10. SGO.PV-2 axis; A, anterior view; B, left lateral view; C, dorsal view. Abbreviations: Bt, big tubercle; Sb, small tubercle; Tl, transverse ligament for holding the odontoid process

The remaining five cervical vertebrae are quite similar. They present a pair of transverse processes with their transverse foramen, a triangular shaped spinous process of moderate size (Owen 1842), and cranial and caudal articular surfaces. Cervical vertebra three (C3) has a spinous process, which is partially covered by the spinous process of the axis. This along with the spinous process of cervical vertebra seven (C7) are the longest of the series (Table 6), although it can be noted that vertebrae's lateral width tends to increase from the third to the seventh vertebra. This is manifested in the width between transverse processes of the cervical vertebrae (Table 6). In fact, the body of the cervical vertebra seven (C7) is clearly greater than the others and is engraved on each side with part of the joint of the first rib (Owen 1842). Additionally, in cervical vertebra seven (C7) there is an absence of the two vertebralarterial canals laterally connected to the vertebral body. This canals are present in all the precedents cervical vertebrae.

b) Dorsal vertebrae

Regarding the preserved eight dorsal vertebrae (T1-T8) it can be stated that their appearance fits previous descriptions remarkably well, with the lateral vertebrae bodies being slightly concave and the spinous processes being inclined slightly along the dorsal region (Owen 1842) (Figure 8). All these vertebrae have in common anterior costal articular surfaces, costal articular surfaces on the transverse processes, and anterior and posterior articular processes. Note that although in the eighth dorsal vertebra from the drawing of Owen (1842: Plate VIII) are presented posterior costal articular surfaces, in the dorsal vertebrae

of the specimen are not present (Figure 8). These surfaces were possibly lost by post mortem erosion processes that are observed posteriorly in the vertebral body. This is confirmed by the fact that ribs have articular surfaces in their head which articulate with these missing surfaces, and that C7 have preserved these posterior surfaces. Another feature to note is the presence of a small foramen in the posterior region of the vertebral body (facing the vertebral foramen), which is present in all dorsal vertebrae (Figures 11 and 12). Given the foramen position, it may be a nutrient canal caused by the connection with the anterior spinal artery through a nutrient artery. Furthermore, a notable difference from the specimen previously described (Owen 1842) is that this specimen has a fusion of the spinous processes of the dorsal vertebrae one and two (T1 and T2) (Figure 11). This fusion occurs at the end of the processes, generating a large extreme that is far superior in magnitude to all others (Table 6). This difference may be due an injury suffered in life, in which the distal tip of T1 broke off causing the fusion between the two. This led to more adhesion with T2 and just marginally repairing itself to T1. However, this event should have happened considerably before the specimen's death provided that there is no clear fracture and ossification line (the fracture observed in Figure 11 A-B is probably the result of a post mortem fracture, and it is not related to the fusion of T1 and T2). Another possibility, is that this specimen could have suffered a congenital deformation of the spinous processes. It would be interesting to observe the same structure in another *Glossotherium* specimens to find out whether it is effectively a pathological trait, or on the contrary, it is a common trait of some biological importance. However, the latter alternative seems unlikely.

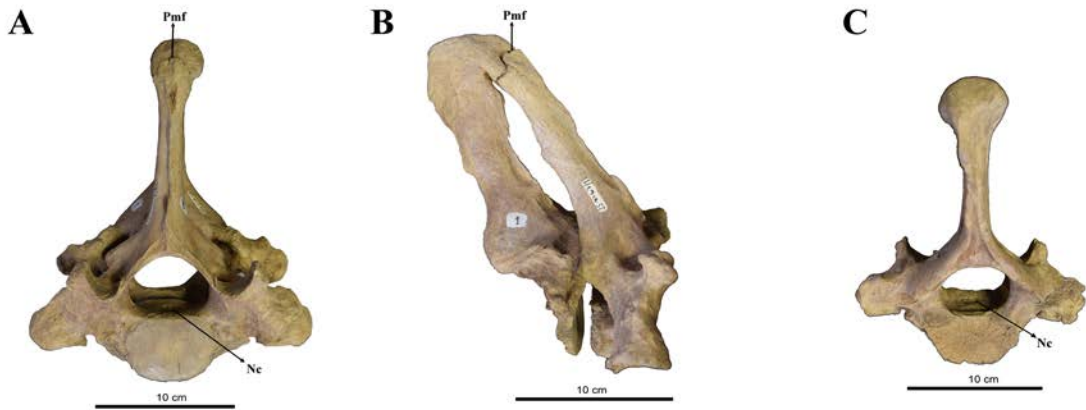


FIGURE 11. Dorsal vertebra one and two (T1 and T2) of SGO.PV.2; A, anterior view; B, right lateral view; C, posterior view. Abbreviation: Nc, Nutrient canal; Pmf, post mortem fracture. Note the fusion of the spinous processes of these vertebrae

Dorsal vertebra one (T1) differs from the subsequent dorsal vertebrae, because it bears cranial articular surfaces similar to cervical vertebrae. Dorsal vertebra two (T2) has a fracture on its right transverse process, and also exhibits damage on the costal articular surface. This vertebra has not conserved all of the posterior region of the body. Dorsal vertebra three (T3) has some anterior marks in the spinous process, suggesting that it was in contact with the fused spinous process of the preceding vertebrae (T1 and T2) but was not fused with them. It also presents damage in the anterior articular surface of the right rib. The last four vertebrae (T5-T8) have the greatest similarity to the drawing of the eighth vertebra of Owen (1842: Plate VIII) in the costal articular surface of their transverse processes. This is because they have a distinct lateral orientation unlike the costal articular surface of the preceding transverse processes which have an anterolateral orientation. Dorsal vertebra five (T5) presents damage in the anterior portion of the body of the vertebra, and dorsal vertebra seven (T7) has most of its spinous process missing by a fracture. When comparing the dorsal vertebrae measurements between SGO.PV.2 and *Paramylodon*, these are very similar, although the later genera tends to be larger (Table 6).

Ribs

Out of the thirty-two ribs which had been previously described (Owen 1842), SGO.PV.2 only preserves fragments of six ribs, which mainly correspond to the head and costal tubercle. The head articulates with the anterior costal articular surface of a vertebra and the posterior costal articular surface of the preceding vertebra, while the tubercle articulates with the costal articular surface of the transverse process of the vertebra. In general, sloths' ribs can be easily distinguished provided that their tubercle has a concave articular surface and the articular surface of the vertebra's transverse process is eminently convex (Fariña *et al.* 2013). This is seen in the ribs and vertebrae of this specimen.

The first fragment corresponds to the left rib of dorsal vertebra one (T1), presenting the head, costal tubercle and the proximal rib body well preserved (Figure 12 A). This articulates perfectly with T1 and C7. The beginning of this rib shaft is more anteriorly oriented than the beginning of the following rib shafts, which are more laterally oriented.

The first fragment corresponds to the left rib of dorsal vertebra three (T3), presenting the head, costal tubercle and the proximal rib body well preserved (Figure 12 B). This articulates perfectly with T3 but not with T2 as it lacks the posterior costal articular surface. The second fragment corresponds to the right rib of T4 presenting the head and costal tubercle well preserved and part of the start of the rib's body (Figure 12 C); posteriorly it shows damage. This articulates perfectly with T4 but not with T3, given its lack of a posterior costal articular surface as in the previous case. The third fragment corresponds to a right rib presenting a well preserved head and costal tubercle and a very minor fraction of the beginning of the rib's body. Since it does not articulate with any of the specimen's preserved vertebrae, it is not possible to know to which rib it corresponds. The fourth fragment is very small and corresponds to a left rib that has the head and part of the tubercle joined by the neck of the rib. The body of this rib was not preserved. The fifth and final fragment corresponds to the left rib, showing a well preserved head, costal tubercle and the proximal rib body. Since it does not articulate with any of the specimen's preserved vertebrae it is hard to tell to which rib it corresponds.

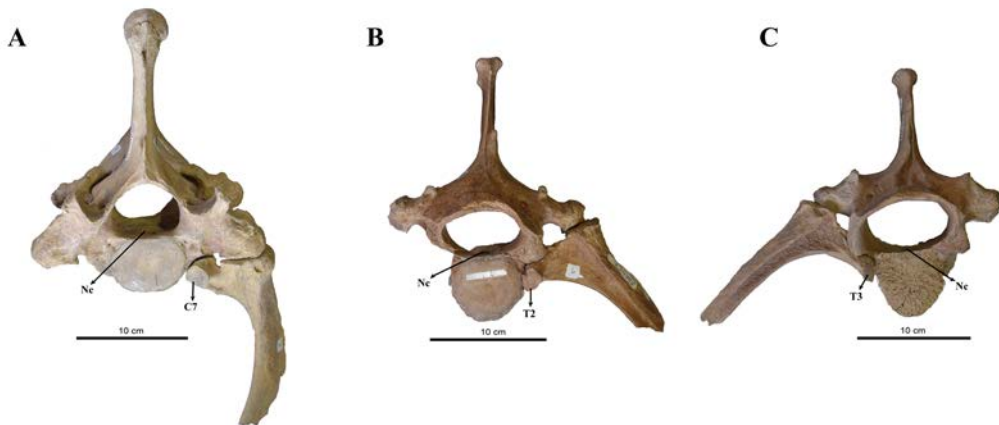


FIGURE 12. A Dorsal vertebra one and two (T1 and T2) of SGO.PV.2, with T1 articulating with a fragment from its left rib in anterior view; B Dorsal vertebra three (T3) of SGO.PV.2 articulating with a fragment from its left rib in anterior view; C Dorsal vertebra four (T4) of SGO.PV.2 articulating with a fragment from its right rib in anterior view. Abbreviations: Nc, Nutrient canal; C7, articular surface for the posterior costal articular surface of cervical vertebra seven; T2, articular surface for the posterior costal articular surface of dorsal vertebra two; T3, articular surface for the posterior costal articular surface of dorsal vertebra three

II) Appendicular skeleton

a) Forelimbs Ulna

There is only one ulna in this specimen and it corresponds to the left one (Figure 13), which is identical to that previously drawn and described by Owen (1842: XI-XIV). Medially, the ulnar shaft presents a smooth concave surface, and laterally a rough irregular surface, possessing a long, large and thick olecranon leaning obliquely. The element is well preserved, with little damage to the olecranon. Laterally, the radial notch that articulates with the head of the radius is ovate and concave like in *Mylodon*. However, it is wider than the latter taxon's one (McAfee 2007, 2016).

The total ulnar length of *Glossotherium* measured from the tip of the olecranon to the surface that articulates with the triquetrum in the distal part of the ulna it is shorter than in *Mylodon* and *Paramylodon* (McAfee 2016). The same is valid for SGO.PV.2, which has very similar measurements to the *Glossotherium robustum* individuals from McAfee (2016; Table 7).

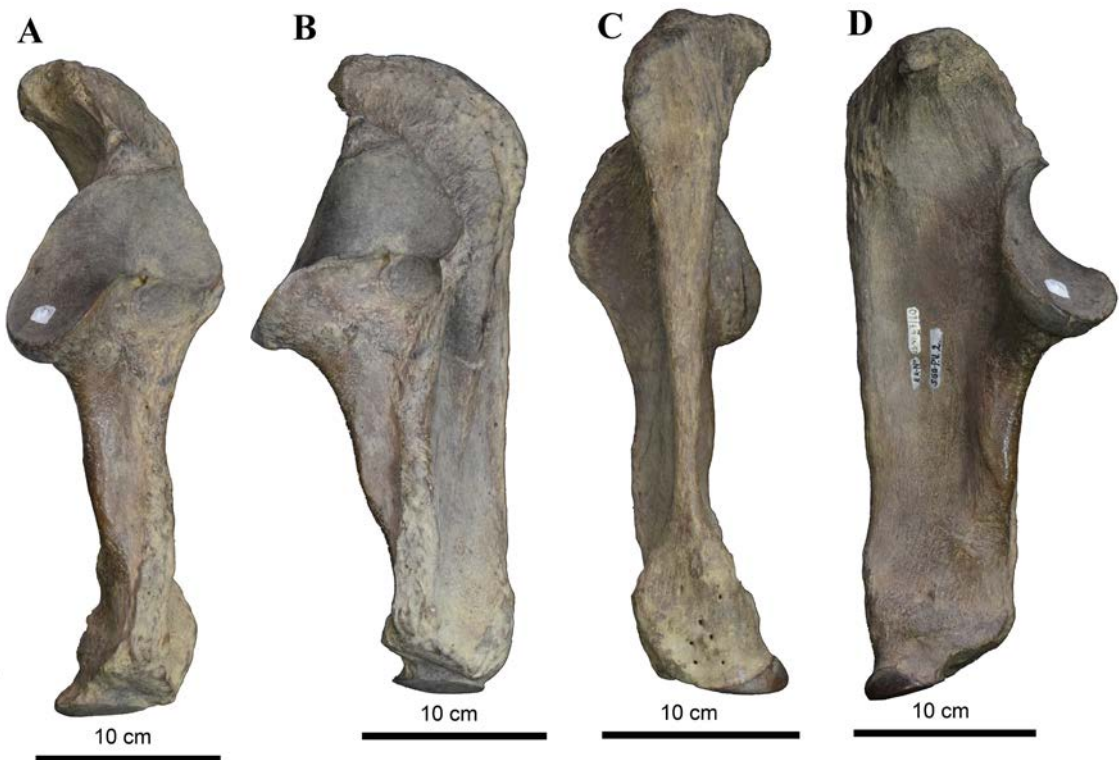


FIGURE 13. SGO.PV.2 left ulna; A, anterior view; B, lateral view; C, posterior view; D, medial view

TABLE 7. Measurements of elements of the forelimbs of SGO.PV.2. All measurements in millimeters and measured at its midpoint whenever were distances between cavities

	SGO.PV.2 (<i>Glossotherium robustum</i>)	<i>Glossotherium robustum</i> (From McAfee 2016)	<i>Paramylodon harlani</i> (From Stock 1925, McAfee 2016)	<i>Myiodon darwinii</i> (From McAfee 2016)
Ulna		N=5	N=12	
Total length	356.9	340.2 ± 12.5	384.1 ± 12.9	372.5
Anteroposterior width at coronoid process	155.3	140.7 ± 7.1	155.7 ± 7.5	141.2
Capitulum length	60.3	74.5 ± 9.4 (N=4)	92.6 ± 4.9	65.9
Trochlea length	104.5	98.9 ± 7.6	118.9 ± 4.3	99.6
Manus bones				
Lunate		-	N=39	
Width between the angle of the capitulum and the scaphoid articular surfaces, and the more proximal angle of the triquetrum articular surface	62.4	-	-	-
Greatest distance from radial surface to face for unciform, measured over dorsal surface	53.8	-	54.3	-
Greatest width across radial surface	64.5	-	66.1	-
Dorsopalmar diameter across unciform facet	52.6	-	51.2	-
First metacarpal (MCC)			N=21	
Proximodistal length (between the articular surface of the scaphoid and the articular surface with the proximal phalanx)	46.0	-	39.8	-
Maximum mediolateral width (between the articular surface with the scaphoid and the articular surface with MC II)	44.8	-	45.8	-
Distal or ungual phalanx (I-3)				
Greatest length (measured from the proximal dorsal end to the tip of the claw)	74.0	-	74.8	-
Depth at proximal end	27.3	-	28.7	-
Distance from subungual tuberosity to dorsal surface of claw-process, measured normal to dorsal border	31.0	-	32.1	-
Greatest width at proximal end	31.1	-	28.9	-
Width of claw-process at distal end of subungual tubercle	17.7	-	15.8	-

(Table 7. Continuation)

	SGO.PV.2 (<i>Glossotherium robustum</i>)	<i>Glossotherium robustum</i> (From McAfee 2016)	<i>Paramylodon harlani</i> (From Stock 1925, McAfee 2016)	<i>Mylodon darwini</i> (From McAfee 2016)
Third metacarpal (MC III)			N=30	
Length, proximodistal	85.2	85.8	103.1	100.2
Proximal height, dorsopalmar	63.2	49.7	69.8	64.4
Shaft depth, dorsopalmar	37.6	30.6	-	29.1
Distal width, mediolateral	50.3	66.9	75.5	64.4
Distal depth, dorsopalmar	56.7	51.9	-	56.4
Ratio of length to distal width	1.694	1.283	1.366	1.556
Greatest width of proximal end	80.0	-	75.5	-
Proximal phalanx three (III-1)			N=40	
Greatest depth	59.7	-	62.7	-
Greatest width	60.0	-	58.0	-
Proximodistal diameter across the lateral surface	30.0	-	39.6	-
Medial phalanx three (III-2)			N=42	
Length measured across middle of inner side	45.0	-	48.9	-
Greatest depth of inner condyle	38.4	-	39.9	-
Depth of proximal end	55.4	-	57.8	-
Greatest width of proximal end	47.0	-	47.9	-

Manus bones

This species has previously been described as pentadactyl, with bones which are wider than they are long, the first three with claws and the last two resembling hoofs (*sensu* Owen 1842). Of the eight bones that would present the carpal bones of an ancient therian (Hall 2008) the carpus of *Glossotherium* presents all of them: the scaphoid, lunate, triquetrum, pisiform, trapezoid, capitate and hamate (unciform), and the metacarpal-carpal complex (MCC), which is the fusion between the trapezium and the first metacarpal (MC I). The MCC was proposed by De Iulis and Cartelle (1994) as an element composed of fused bones present medially in the manus of many Tardigrada, based on observations made in *Megatherium* and *Eremotherium*. This formalization was made mainly to rectify a misunderstanding, first by Cuvier (1823) and then by Owen (1842, 1851) in the description of the manus of *Megatherium americanum* and *Glossotherium robustum*. They believed that the MCC was a fusion between the scaphoid with the trapezium, shared with *Choleopus*. However, in the following years different studies (Humphry 1870, Flower 1873, 1885, Menegaux 1908, 1909a, b, Poche 1908, 1911) suggested that the trapezium was fused to the MC I. In mylodontids, Stock (1925) observed that a few specimens of *Paramylodon harlani* had the trapezium and the MC I, which confirm the suggested origin of the MCC in a taxon very akin to *Glossotherium robustum*.

Of the five metacarpals that would have the ancestral therian (Hall 2008), this species has all of them (MC I-V). Of the four fingers with three phalanges and a thumb with two phalanges, this species would have all except for the digits four and five which have only two phalanges instead of three. In

SGO.PV.2 only seven bones of this portion were preserved which broadly coincide with the drawings and descriptions of Owen (1842). For clarity, the MCC is going to be mentioned within the metacarpal bones, although as explained before it should be also considered within the carpal bones.

Regarding the carpal bones, only the left lunate was preserved (Figure 14) and it coincides exactly with previous descriptions (Owen 1842) as it resembles more closely a wedge than a half-moon, and being much thicker dorsally than palmarly. It has six sides and articular surfaces for the radius, the scaphoid, the triquetrum, the hamate or unciform, and the capitate. The most noteworthy and largest of these surfaces is the radius articular surface, which forms a semicircular convex curve. When comparing the lunate measurements between SGO.PV.2 and *Paramylodon*, these prove to be remarkably similar (Table 7).

Regarding the metacarpal bones, only the left MCC, the right MCC, and the third left metacarpal (MC III) were preserved. Associated with the left MCC is the distal phalanx (I-3) of the same digit, and associated with the left MC III are the proximal (III-1) and medial phalanges (III-2) of the same digit. Regarding the first digit, the MCC fits with previous descriptions (Figure 15 A-F) presenting two proximal articulations, one with the scaphoid and the other with the terminal end of the second metacarpal, and a distal articulation which articulates with the proximal phalanx (Owen 1842). As described for *Glossotherium* and *Paramylodon* (McDonald 1987), the articular surface for the scaphoid in SGO.PV.2 is almost flat but slightly convex dorsopalmarly (Figures 15 C and E), in contrast with *Myiodon* which is axioabaxially concave and slightly convex dorsopalmarly (Haro *et al.* 2016). Additionally, SGO.PV.2 lacks a small trapezoid articular facet laterally as it was described for *Glossotherium* and *Paramylodon* (McDonald 1987; Stock 1925), in contrast with *Myiodon* which presents this facet (Haro *et al.* 2016). Although the appearance of the MCCs

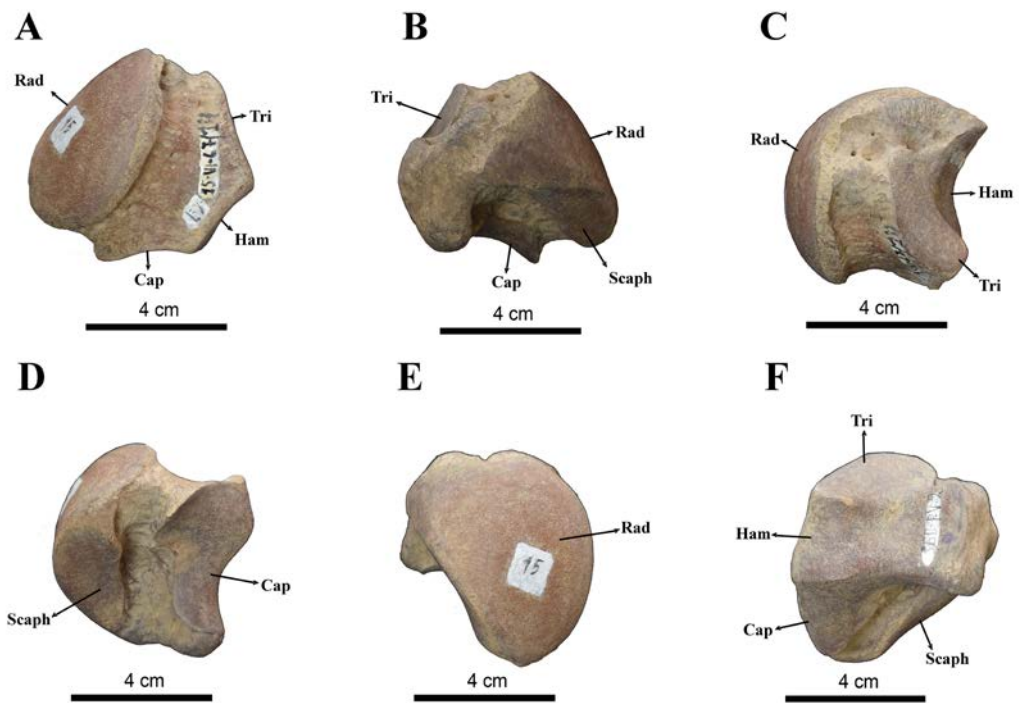


FIGURE 14. SGO.PV.2 left lunate; A, dorsal view (proximal towards top, medial towards left), B, palmar view (proximal towards top, medial towards right), C, proximal view (dorsal towards bottom, medial towards left), D, distal view (dorsal towards bottom, medial towards left), E, medial view (dorsal towards right, proximal towards top), F, lateral view (dorsal towards left, proximal towards top); Abbreviations: Rad, radius; Tri, triquetrum; Ham, hamate; Cap, capitate; Scaph, scaphoid

is nearly identical with those of *Paramylodon harlani* (Allen 1913), these elements are longer and slightly narrower in SGO.PV.2 (Table 7) when compared to the *Paramylodon harlani* specimens of Stock (1925). The right MCC represents a mirror image of the left one. In both MCCs of SGO.PV.2 there is a transverse groove with depth on the palmar side (Figure 15 B), which although mentioned in Owen's description (1842) does not appear in his drawings (Owen 1842: Plates XV and XVI). The transverse groove could be a variable feature within *Glossotherium* individuals and it may be associated to the fusion between the trapezium and MC I, because of its location between these two bones. A similar feature, described as a partially fused suture between trapezium and MC I has been characterized palmarly in the same area for *Myiodon* (Haro *et al.* 2016). The associated I-3 (Figure 15 G-L), in palmar view, has a double articular surface proximally which articulates with the proximal phalanx (I-1) that has two major vascular foramina

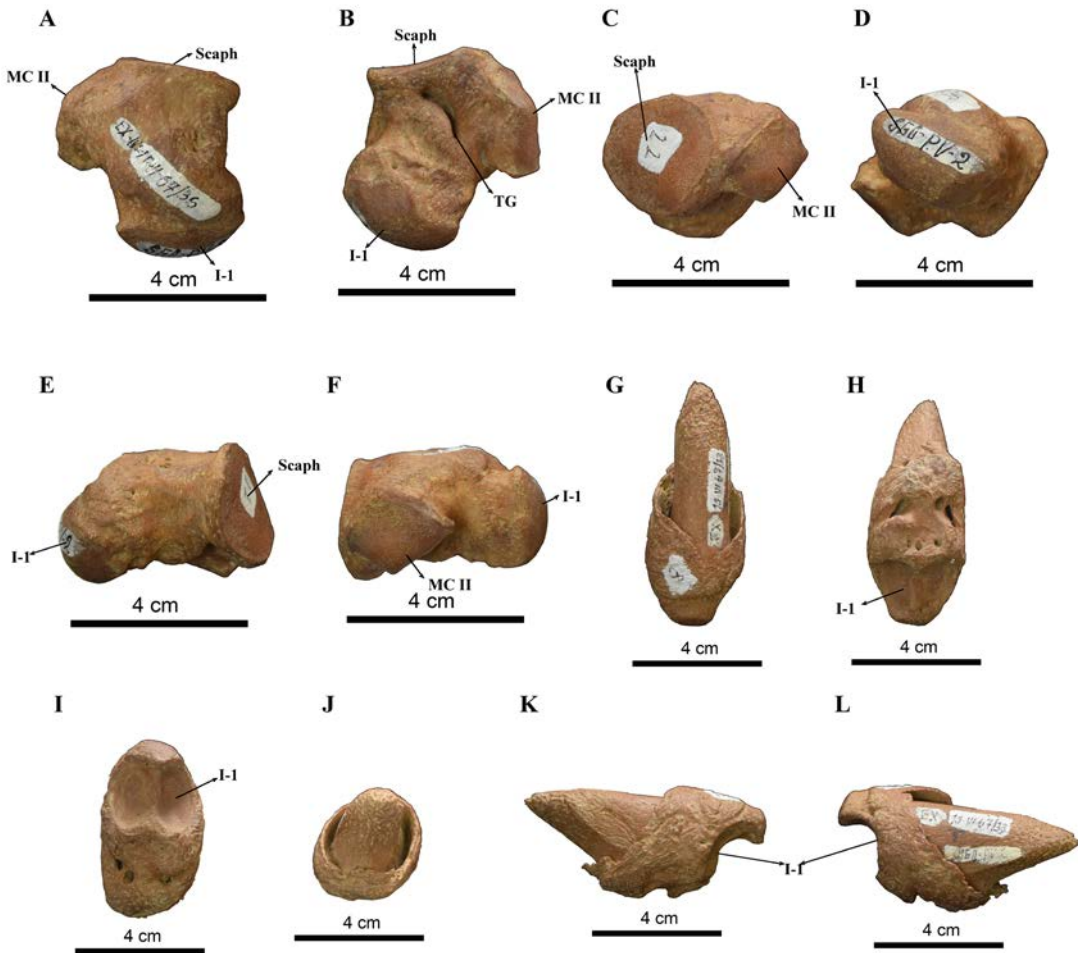


FIGURE 15. A-F SGO.PV.2 right metacarpal-carpal complex (MCC); A, dorsal view (proximal towards top, medial towards right), B, palmar view (proximal towards top, medial towards left), C, proximal view (dorsal towards top, medial towards left), D, distal view (dorsal towards top, medial towards right), E, medial view (dorsal towards top, proximal towards right), F, lateral view (dorsal towards top, proximal towards left); G-L SGO.PV.2 left distal/ungual phalanx of the digit one (I-3); G, dorsal view (proximal towards bottom, medial towards right), H, palmar view (proximal towards top, medial towards left), I, proximal view (dorsal towards top, medial towards right), J, distal view (dorsal towards top, medial towards left), K, medial view (dorsal towards top, proximal towards right), L, lateral view (dorsal towards top, proximal towards left). Abbreviations: Scaph, scaphoid; MC II, metacarpal II; I-1, proximal phalanx of digit I; Tg, transverse groove

a bit distally (Figure 15 H). Dorsally, there is a bony collar surrounding a claw (Owen 1842; Figure 15 G). Although, the I-3 of SGO.PV.2 shows measurements which are very similar to those of *Paramylodon* (Table 7), they are slightly wider mediolaterally.

In relation to the third digit (Figure 16), the left MC III (Figure 17 A-D) also fits with previous descriptions (Owen 1842: Plates XV and XVI), shaped as a “T”, with proximal articular surfaces for the capitate, hamate (unciform), and the second and fourth metacarpals (MC II and MC IV). The smaller medial articular surface for the capitate (Figure 17 A) is more rounded at the corners and slightly concave in *Glossotherium* and *Paramylodon* in contrast to *Myiodon*, in which this articular surface is flat (McAfee 2016). In addition to that, and as described for *Glossotherium*, SGO.PV.2 presents only one MC IV (Figure 17 D) articular surface in contrast with *Myiodon*, which presents two MC IV facets, a dorsal one and a palmar one (McAfee 2016). However, this feature could be variable in mylodontids because Haro *et al.* (2016) described a single facet for MC IV in *Myiodon*, and McDonald (1987) describes two facets for MC IV in *Glossotherium* and *Paramylodon*. Stock’s drawings (1925: Fig. 84 A) agree with the two facets for MC IV in *Paramylodon*. The MC III greatest width is between the articular surfaces with adjacent metacarpals and its greatest length is from the articular surface of the capitate to the distal end, wherein it has an articular surface that articulates for the proximal phalanx (III-1).

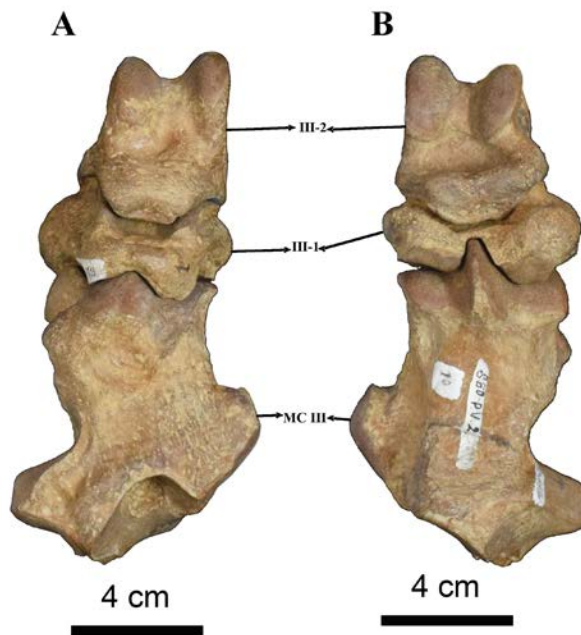


FIGURE 16. Third digit of the left forefoot of SGO.PV.2; A, dorsal view (proximal towards bottom, medial towards right), B, palmar view (proximal towards bottom, medial towards left). To complete the digit, the distal phalanx (III-3) of the same digit would be needed. Abbreviations: MC III, metacarpal III, III-1, proximal phalanx of digit III, III-2, medial phalanx of digit III

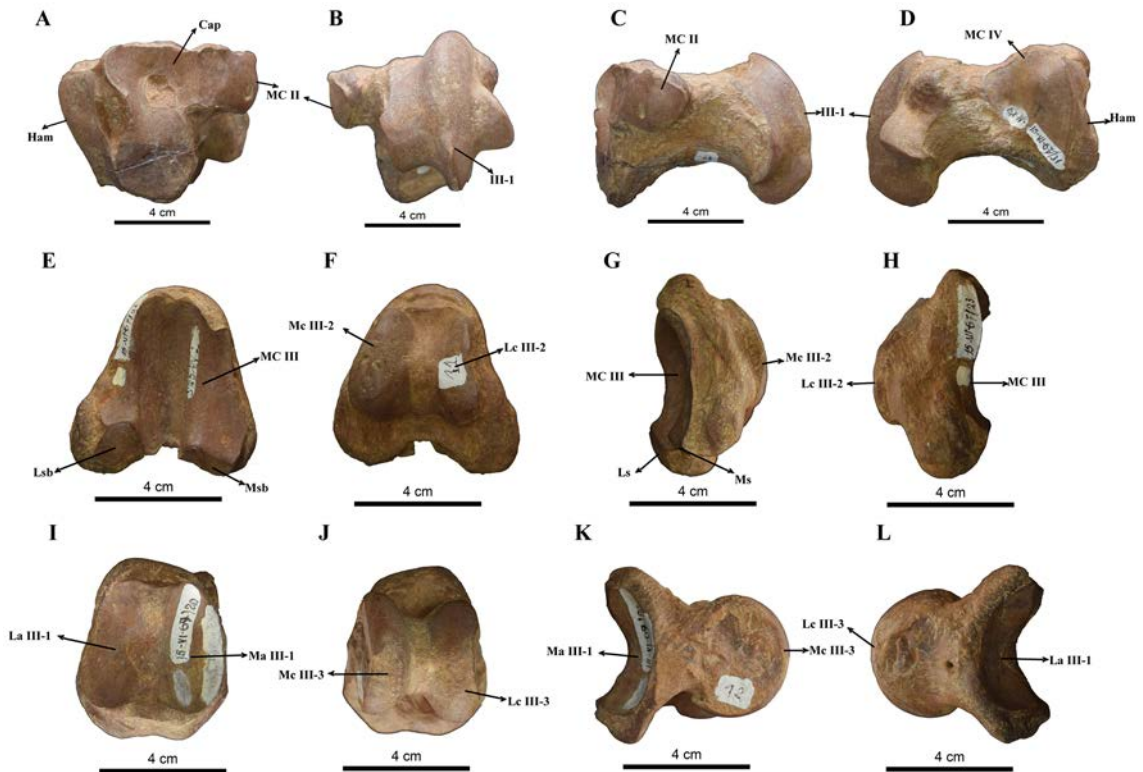


FIGURE 17. A-D SGO.PV.2 left metacarpal three (MC III); A, proximal view (dorsal towards top, medial towards right), B, distal view (dorsal towards top, medial towards left), C, medial view (dorsal towards top, proximal towards left), D, lateral view (dorsal towards top, proximal towards right); E-H SGO.PV.2 left proximal phalanx of digit three (III-1); E, proximal view (dorsal towards top, medial towards right), F, distal view (dorsal towards top, medial towards left), G, medial view (dorsal towards top, proximal towards left), H, lateral view (dorsal towards top, proximal towards right); I-L SGO.PV.2 left medial phalanx of digit three (III-2); I, proximal view (dorsal towards top, medial towards right), J, distal view (dorsal towards top, medial towards left), K, medial view (dorsal towards top, proximal towards right), L, lateral view (dorsal towards top, proximal towards right). Abbreviations: Ham, hamate; Cap, capitate; MC II, metacarpal II; MC IV, metacarpal IV; Lsb, lateral sesamoid bone; Msb, medial sesamoid bone; Mc III-2, medial condyle for III-2; Lc III-2, lateral condyle for III-2; La III-1, lateral articular surface for III-1; Ma III-1, medial articular surface for III-1; Mc III-3, medial condyle for III-3; Lc III-3, lateral condyle for III-3

When comparing SGO.PV.2 MC III dimensions with other mylodontids (Table 7), they are closer to those of the *Glossotherium robustum* individual (from McAfee 2016). The greatest difference between *Glossotherium robustum* and the other two species, *Mylodon* and *Paramylodon*, is its shorter proximodistal length. The distal dorsopalmar depth or height is very similar between SGO.PV.2 and *Mylodon*, contrary to McAfee (2016) observations of a distal height much greater in *Mylodon* than *Glossotherium*. So, this feature is variable and it is not the most appropriate to distinguish both genera.

The III-1 is very short, as in most of Xenarthra, being much larger vertically (Figure 17 E-H). Proximally, it has a concave articular surface with a deep median groove for MC III (Figure 17 E) and distally a convex articular surface (Figure 17 F) with two condyles separated by an extensive groove that articulates with the medial phalanx (III-2). Palmarly, it has two articular surfaces for sesamoid bones (Figure 17 E and G). The measurements of this element in SGO.PV.2 are very similar to those of *Paramylodon*, although the proximodistal diameter across the lateral surface is larger in *Paramylodon* (Table 7).

The III-2 is longer than the previous element (Figure 17 I-L). As the proximal phalanx, it has two main articular surfaces that articulate with it: a concave one, with two facets separated by a ridge in the middle for the proximal phalanx (Figure 17 I) and a convex one, with a median groove separating two articular condyles (Figure 17 J) that articulate with the distal or ungual phalanx (III-3), which was not preserved in this specimen. When comparing the SGO.PV.2 III-2 with that of *Paramylodon*, the former is slightly smaller in all measurements (Table 7).

b) Hindlimbs

Hindfoot bones

The feet of *Glossotherium robustum* are tetradactyl (digit one was lost), possessing digits in close analogy to the manus, with the first two bearing great claws and the last two resembling hoofs (Owen 1842). Of the seven bones that would be present in the tarsus of an ancestral therian (Hall 2008), the tarsus of this species has six bones: talus, calcaneus, navicular, cuboid, and only two of the cuneiform bones, the second or intermediate, here medial, and the third or lateral. In addition, this species has four metatarsals (MT II-V) with three phalanges each on the first two, and only two phalanges each on the last two digits. In SGO.PV.2 only seven bones of this portion were preserved (Figures 18, 19 and 20), which in general terms are fully consistent with the descriptions and drawings of Owen (1842: Plates XXI-XXIII).

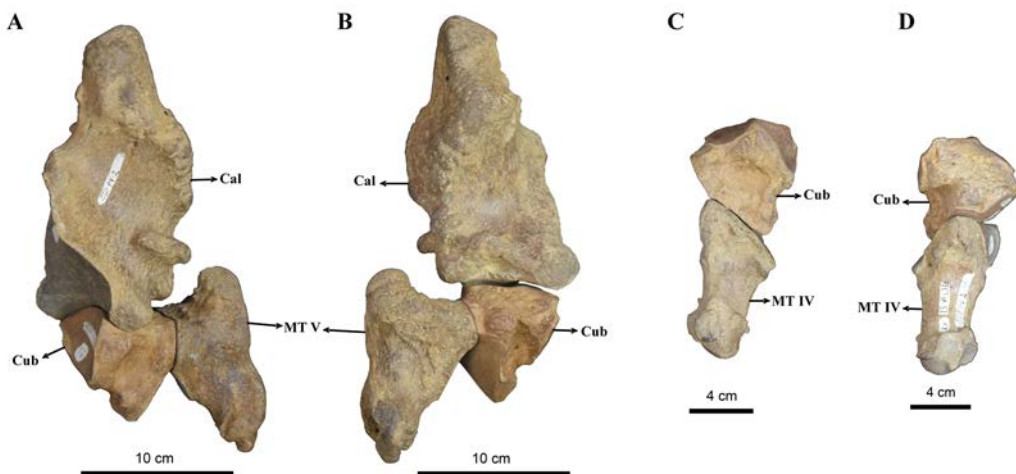


FIGURE 18. A-B SGO.PV.2 calcaneus, cuboid and fifth metatarsal of its left hindfoot; A, dorsal view (proximal towards top, medial towards left), B, plantar view (proximal towards top, medial towards right); C-D SGO.PV.2 cuboid and fourth metatarsal of its right hindfoot; C, dorsal view (proximal towards top, medial towards right), D, plantar view (proximal towards top, medial towards left). Abbreviations: Cal, calcaneus; Cub, cuboid; MT V, metatarsal V; MT IV, metatarsal IV

Concerning the tarsus only the left calcaneus, left cuboid, right cuboid, right astragalus and third or lateral cuneiform were preserved. The calcaneus matches previous descriptions exactly, having a rough posterior portion which is very large in width and length, and has a wide and concave triangular base (Owen 1842; Figures 18 A-B and 19 A-C). It has two articular surfaces, a superior one holding the astragalus and another one in the anterior end which articulates with the cuboid. It also has in its posterior end small and medium, probably vascular, foramina. The measurements of these elements in SGO.PV.2 are considerably smaller to those of *Paramylodon* (Table 8).

The cuboid coincides with previous descriptions, being short and wide with well demarcated articular sections on which six different bones articulate (Owen 1842) (Figures 18 C-D and 19 D-G). Proximally, the cuboid articulates the calcaneus and medial distally the astragalus and navicular. Lateral

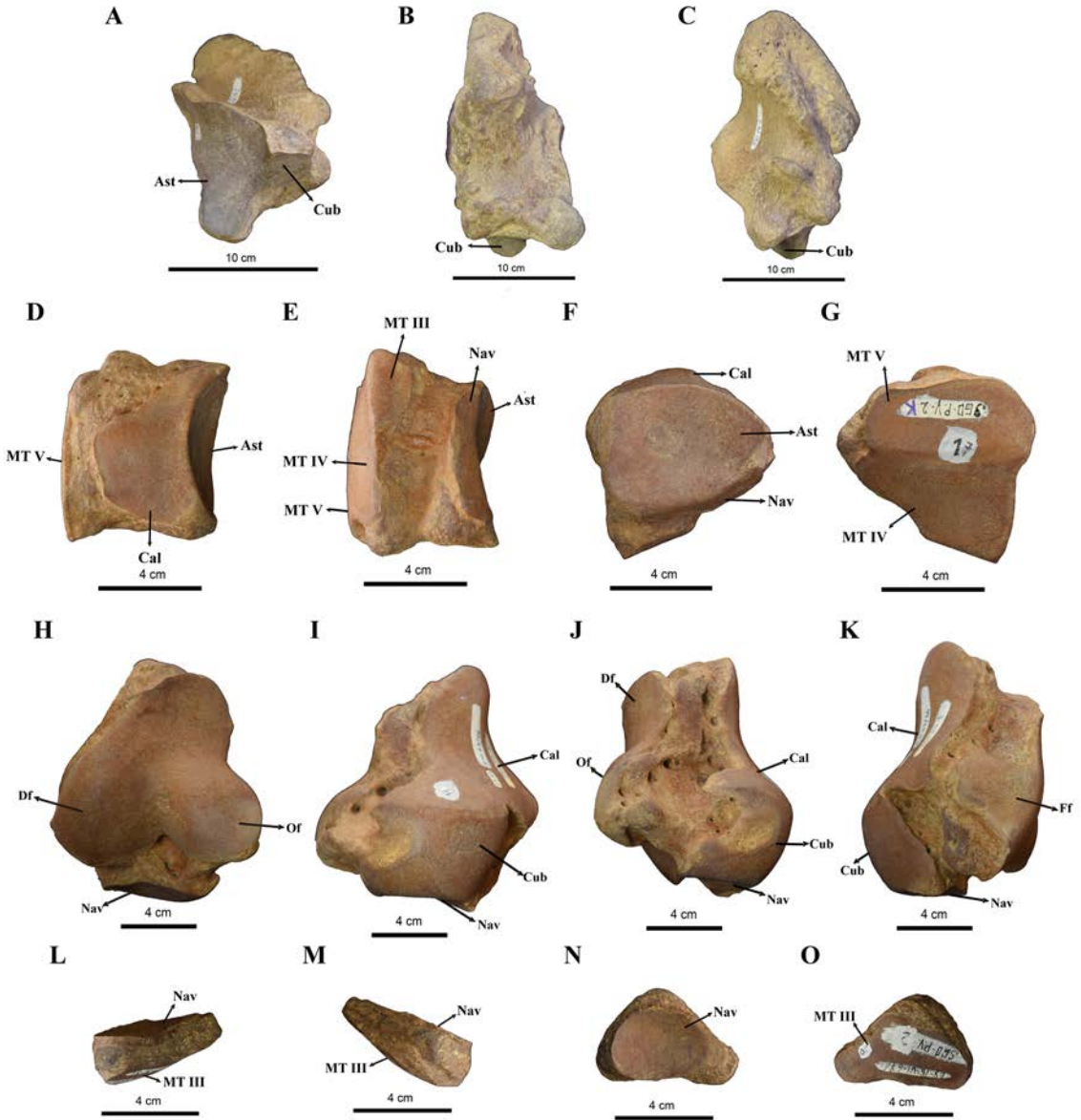


FIGURE 19. A-C SGO.PV.2 left calcaneus; A, proximal view (dorsal towards top, medial towards left), B, medial view (dorsal towards right, proximal towards bottom), C, lateral view (dorsal towards left, proximal towards bottom); D-G SGO.PV.2 right cuboid; D, proximal view (dorsal towards bottom, medial towards right), E, distal view (dorsal towards top, medial towards right), F, medial view (dorsal towards left, proximal towards top), G, lateral view (dorsal towards right, proximal towards top); H-K SGO.PV.2 right astragalus; H, dorsal view (proximal towards top, medial towards right), I, plantar view (proximal towards top, medial left), J, medial view (dorsal towards left, proximal towards top), K, lateral view (dorsal towards right, proximal towards top); L-O SGO.PV.2 third left cuneiform; L, dorsal view (proximal towards top, medial towards left), M, plantar view (proximal towards top, medial towards right), N, proximal view (dorsal towards bottom, medial towards left), O, distal view (dorsal towards bottom, medial towards right). Abbreviations: Ast, astragalus; Cub, cuboid; Cal, calcaneus; MT III, metatarsal III; MT IV, metatarsal IV; MT V, metatarsal V; Nav, navicular; Df, discoid facet; Of, odontoid facet; Ff, fibular facet

distally, the cuboid articulates the fourth and fifth metatarsals (MT IV and V), and distally it articulates the third metatarsal (MT III). Each cuboid is a mirror image of the other one. When comparing the dimensions of the cuboid of SGO.PV.2 with *Paramylodon* (Table 8), the former has greater values in all the measurements. Therefore, it is probable that this element is bigger in *Glossotherium* than in *Paramylodon*.

However, the proportions between the measurements within each genus are quite similar, so it is plausible that despite *Glossotherium*'s cuboid being bigger, the shape of this element could be very similar to that of *Paramylodon*.

TABLE 8. Measurements of hindfoot bones of SGO.PV.2. All measurements in millimeters and measured at its midpoint whenever were distances between cavities

	SGO.PV.2 (<i>Glossotherium</i> <i>robustum</i>)	<i>Paramylodon harlani</i> (From Stock 1925, McAfee 2016)
Calcaneus		N=21
Anteroposterior length	190.4	224.8
Greatest width across inferior side of posterior expansion	117.2	123.9
Least width across inferior side of neck	46.7	60.2
Greatest width at anterior end, measured across astragalar surface	86.1	91.8
Greatest depth, measured across outer side	103.5	125.4
Cuboid		N=32
Proximodistal diameter through middle	65.4	54.3
Dorsopalmar diameter through middle	62.4	55.3
Greatest transverse diameter along metapodial border of dorsal surface	86.5	71.3
Astragalus		N=41
Anteroposterior diameter	130.0	140.2
Greatest distance from fibular facet to cuboid-navicular surface across front depression	103.6	104.4
Greatest distance from end of fibular facet to end of ascending process with inner tibial surface	117.0	134.3
Distance from fibular border of lateral tibial surface to navicular surface	104.1	115.3
Anteroposterior extent of lateral tibial surface	101.3	121.4
Third or lateral cuneiform		N=30
Greatest dorsoplantar diameter	44.4	58.9
Greatest width	58.3	44.8
Greatest depth of dorsal face	22.0	29.8
Fourth metatarsal (MT IV)		N=29
Greatest length measured along outer side close to dorsal border	107.0	119.3
Greatest depth of proximal end measured along proximal border	62.0	60.7
Greatest width of proximal end	53.4	45.5
Least width of shaft	34.9	36.3
Least depth of shaft	24.2	27.0
Depth of distal end	59.2	50.1
Width of distal end	39.6	43.5

(Table 8. Continuation)

	SGO.PV.2 (<i>Glossotherium robustum</i>)	<i>Paramylodon harlani</i> (From Stock 1925, McAfee 2016)
Fifth metatarsal (MT V)		N=26
Length from proximal border of cuboid facet on distal extremity	104.1	113.9
Dorsoplantar distance measured along ridge separating cuboidal surface from facet for metatarsal IV	60.8	70.7
Distance from surface for metatarsal IV to end of lateral tuberosity	71.9	76.4
Anteroposterior length from the large protuberance to the distal articular surface for the proximal phalanx.	128.3	-

FIGURE 20. A-D SGO.PV.2 fourth right metatarsal (MT IV); A, proximal view (dorsal towards bottom, medial towards right), B, distal view (dorsal towards top, medial towards right), C, medial view (dorsal towards left, proximal towards top), D, lateral view (dorsal towards right, proximal towards top); E-H SGO.PV.2 fifth left metatarsal (MT V); E, proximal view (dorsal towards bottom, medial towards left), F, distal view (dorsal towards top, medial towards left), G, medial view (dorsal towards right, proximal towards top) H, lateral view (dorsal towards left, proximal towards top). Abbreviations: Cub, cuboid; MT III, metatarsal III; MT IV, metatarsal IV; MT V, metatarsal V; IV-1, proximal phalanx of MT IV; V-1, proximal phalanx of MT V

Moreover, the right astragalus exactly matches previous descriptions in having an irregular pyramidal shape with three tubercles on its dorsal surface which articulate with the articular surface of the tibia, and laterally to this surface, there is the articular surface with the fibula (Owen 1842; Figure 19 H-K). Plantarly, there is a large elongated articular surface adapted to the calcaneus and cuboid, and anteriorly for the navicular. Between the articular surfaces it presents many, probably vascular, foramina. As in *Paramylodon*, the astragalus does not present a channel or articular furrow between the discoid and odontoid facets of the tibial articulation, in contrast with *Mylodon* (McAfee 2016). When comparing the dimensions of SGO.PV.2 astragalus with *Paramylodon* (Table 8) this element is smaller in all the measurements.

Finally, the third or lateral left cuneiform is consistent with previous descriptions (Owen 1842) presenting a very compressed anteroposteriorly triangular shape which is wider laterally (Figure 19 L-O). It has only two articular surfaces, a concave one for the navicular, and another one that is slightly convex to the third metatarsal. This element in SGO.PV.2, although wider, is smaller compared with *Paramylodon* in other measurements (Table 8).

Regarding the metatarsals, just the fourth right metatarsal (MT IV) and fifth left metatarsal (MT V) were preserved (Figures 18 and 20), which happen to be the largest in this species. The fourth right metatarsal (MT IV) fully agrees with previous descriptions (Owen 1842) (Figures 18 C-D and 20 A-D), posteriorly having a large articular surface separated into two sections by a sharp angle, with the outer or lateral surface being the one that articulates with the fifth metatarsal, while the inner or medial surface proximally articulates with the cuboid and distally with the third metatarsal. Anteriorly, it has a vertically elliptical articular surface which is narrow and convex to articulate with the fourth proximal phalanx. Plantarly, there are two small recesses for two sesamoid bones. When comparing the dimensions of SGO.PV.2 MT IV with *Paramylodon* (Table 8), this element is shorter but wider in SGO.PV.2 than in *Paramylodon*.

The fifth left metatarsal (MT V) also coincides with previous descriptions being of large size and strength, and proximally having in the medial face a large articular surface divided into two sections by an angle, one that articulates with the cuboid, and the other that articulates with the fourth metatarsal (MT IV) (Owen 1842; Figures 18 A-B and 20 E-H). Proximally, in the exterior or lateral side it has a large rough protuberance separated from the articular surface by a concavity. A surface at the proximal end indicating an articulation between the fifth metatarsal (MT V) and calcaneus for *G. robustum* has been described by Stock (1925). As in the case of *Paramylodon*, this articulation is not present in SGO.PV.2. Distally, it has a vertically elliptical convex articular surface with the proximal phalanx ending palmarly in small concavities for two sesamoid bones separated by a short convex edge. Laterally, on this section it has a small fracture with some erosion. The MT V of SGO.PV.2 is smaller than the one of *Paramylodon* in all the measurements (Table 8).

The manner in which the fifth metatarsal articulates makes it the weight-bearing element in contact with the substrate (Owen 1842). This feature is associated with the unique pedolateral arrangement described in several sloths (nothrotherids, scelodotherids and mylodontids) where there is a rotation of the hind foot, so that the foot plant takes a rather medial position only contacting the ground with the fifth metatarsal and the calcaneus (Fariña *et al.* 2013).

DISCUSSION

Regarding the PCA results from the first analysis with the dataset of McAfee (2007, 2009), it is possible to observe that they are consistent with the results obtained by the same author, thus showing a strong separation between *Glossotherium robustum* and *Paramylodon harlani* (Figure 3). Concerning the LDA, and using the same dataset, SGO.PV.2 was classified as a specimen of *Glossotherium robustum* when applying the obtained discriminant function (Table 2). The location of SGO.PV.2 within the 95% confidence interval for *Glossotherium robustum* in this PCA is consistent with the previous diagnosis of this individual based on McAfee (2007, 2009). The PCA results obtained using the Pitana *et al.* (2013) dataset showed a separation between two groups of *Glossotherium* (Figure 4). The SGO.PV.2 specimen was located again within the *Glossotherium robustum* 95% confidence interval. Therefore, this specimen could be considered as a representative of the southernmost species, which is coincident with the location of its discovery in

Lonquimay, Chile. This is also supported by the classification of SGO.PV.2 as a specimen of *Glossotherium robustum* by the obtained discriminant function in the second LDA as well (Table 4). However, the results both LDA analyses should be treated with caution given the small sample sizes. In addition, the obtained phylogeny placed SGO.PV.2 in close relation to *Glossotherium*, which according to our interpretation indicates that the former belongs to that genus (Figure 5). Considering all the results, it is possible to confirm the previous taxonomic diagnosis establishing the SGO.PV.2 specimen as a *Glossotherium robustum* individual (Labarca 2015). Further analyses could ratify this adscription by either increasing the comparative sample size and/or carrying out ancient DNA analyses.

The description of the postcranial elements of SGO.PV.2 is consistent with the most detailed description to date of these elements from *Glossotherium robustum* found in Owen (1842), and agrees with McAfee (2016) that in general terms the postcranial measurements of *Glossotherium* are smaller than *Myiodon* and *Paramyiodon*, being the last one the largest of these three genera (Tables 5-8). These differences are very remarkable in some limb bones as the ulna and the radius (McAfee 2016). However, some anatomical elements of *Glossotherium* do not exhibit truly noticeable differences, showing similar sizes with the other two genera or even surpassing them. Therefore, when comparing different anatomical elements between these genera, it is always recommended to analyze them in a case-by-case basis.

The finding of SGO.PV.2 and its identification as a *Glossotherium robustum* specimen has a great importance since this specimen is the only record of this species in Chile. The location of the finding (Figure 1) at 23 km from the Lonquimay town and near to Pino Hachado border (38°S) also highlights the importance of the Andean mountain passes (trasandean corridors) as migration routes between the Chilean and Argentinean flora and fauna (Casamiquela 1968, Moreno *et al.* 1994). It is unclear whether the crossing of *Glossotherium robustum* individuals from the Argentinean Patagonian steppe was sporadic or a common event that led to the establishment of populations of this species in Chile, since further research is required. Another possibility, not previously considered, is the migration of *Glossotherium robustum* through the Pacific coast (*i.e.* southward from northern Chile and southern Peru and Bolivia) or through desertic corridors as proposed for other Folivora species such as *Megatherium medinae* and *Scelidodon chiliense* (Moreno *et al.* 1994). In fact, the fossil record shows the unequivocal presence of *Glossotherium robustum* in the coastal regions of Peru (Pujos and Salas 2004) and according to Esteban (1996) its presence in Bolivia. In Chile, several mylodontid dermal osteoderms have been found in coastal areas in northern Chile, as the different superficial deposits of Los Vilos District (~31°S), like the Quebrada Quereo (Núñez *et al.* 1994a) and El Avistadero sites (Seguel *et al.* 2010), and in central Chile in sites such as GNL Quintero 1 (GNLQ1), in the Quintero Bay (32°S; Cartajena *et al.* 2013). Additionally, some dermal osteoderms have been found in the central valley of Chile in Tagua Tagua basin (34°S; Casamiquela 1976, Moreno *et al.* 1994, personal observation). In two of these sites (*i.e.* El Avistadero and GNLQ1) mylodontid distal phalanxes were also found. Interestingly, the Quebrada Quereo (Núñez *et al.* 1994a) and the Tagua Tagua (Núñez *et al.* 1994b) sites, preserved remains associated to human presence. Apparently, in all the above-mentioned sites there were similar environmental conditions during the Pleistocene, which were wetter and colder when compared to present times (Núñez *et al.* 1994a). These conditions favored the congregation of diverse species around resource concentrated areas such as streams, lagoons, estuaries, fertile plains and wetlands (Núñez *et al.* 1994a,b, Mendez 2004, Jackson *et al.* 2007, Cartajena *et al.* 2013). Nevertheless, it is important to consider that these osteoderms could not only belong to *Glossotherium robustum*, but could be from other mylodontid Pleistocene species such as *Myiodon darwinii* and *Scelidodon chiliense*. In fact, in one of the superficial deposits of Los Vilos District, the Quebrada Lazareto site (~31° 50'S), two postcranial bone fragments were assigned to *Myiodon* sp. (Jackson *et al.* 2005). Another source of support for the hypothesis regarding a possible *Glossotherium robustum* migration route along the Pacific coast comes from Varela and Fariña (2016). They generated species distribution models for the last interglacial (LIG), the global last glacial maximum (LGM) and the Holocene climatic optimum (HCO) for three extinct South American Pleistocene mylodontid ground sloths, *Glossotherium robustum*, *Lestodon armatus* and *Myiodon darwinii*. The predicted potential distribution during the LGM for *Glossotherium robustum* showed areas of high prob-

ability in some regions of the Pacific coast of Ecuador, Peru, and north and central Chile (Varela and Fariña 2016). High probability areas occur on exposed areas of the continental shelf that are now submerged, due to a lower sea level during LGM as in the GNLQ1 site (Cartajena *et al.* 2013). However, a similar coastal potential distribution during LGM was also predicted for *Myiodon darwini* (Varela and Fariña 2016). Remarkably, a stable isotope analysis ($\delta^{13}\text{C}_{\text{ap}}$ and $\delta^{18}\text{O}_{\text{ap}}$) on the bioapatite of the mylodontid remains dated in 25,574-25,202 calibrated years BP from the GNLQ1 site, showed mainly C3 plants consumption (López *et al.* 2016). This dietary pattern is like the one observed in Late Pleistocene *Glossotherium robustum* remains from the Buenos Aires Province (Barrientos 1999, Czerwonogora *et al.* 2011, Prado *et al.* 2015, Bocherens *et al.* 2016, Bocherrens *et al.* 2017). Although it is relevant to bear in mind that a similar dietary pattern was observed in some Late Pleistocene bone collagen samples from *Myiodon darwini* (Steele and Politis 2009, Prevosti and Martin 2013). All this evidence suggests that during the Pleistocene, the coastal areas of north and central Chile were occupied by *Glossotherium robustum* and/or *Myiodon darwini*, and that this distribution could be explained by a southward migration of these taxa along the Pacific coast from Peru. It is possible that this migration arrived as far south as Lonquimay (38°S). However, the absence of unequivocal *Glossotherium robustum* specimens in north and central Chile, and its completely absence further south from Tagua Tagua (34°S), is more consistent with the transandean corridor hypothesis (Casamiquela 1968, Moreno *et al.* 1994). Although *Glossotherium robustum* may have permanently inhabited the area during the late Pleistocene in Lonquimay, its presence did not necessarily mean an expansion and occupation of other regions of the country starting from there. Even if there were suitable areas for *Glossotherium robustum* in the coastal areas of north and central Chile (Varela and Fariña 2016), the different bioclimatic variables from the eastern and western sides of the Andes at the level of Lonquimay, probably generated great differences in the vegetation at both sides of the Cordillera that possibly acted as an ecological barrier to dispersal (Casamiquela 1969). However, considering all the available evidence, it is still not possible to discard the southward migration of *Glossotherium robustum* along the Pacific coast from Peru to Chile.

CONCLUSIONS

The analyses of the SGO.PV.2 skull as well as its postcranial skeleton description, confirm the presence of *Glossotherium robustum* in the Pleistocene of Lonquimay. This has a great importance as this is the only record of this species in Chile. Future studies should increase the sample sizes and consider more cranial measurements, including features that were only qualitatively described by Pitana *et al.* (2013) but that were not included in the PCA. Thus, after correcting for size influence, it will be possible to compare more aspects of the skull related to its shape.

The description of SGO.PV.2 postcranial remains, excepting slight variations that could be considered as intraspecific for *Glossotherium robustum*, is coincident with Owen (1842).

The location of this *Glossotherium robustum* specimen finding in Lonquimay (38°S) could be explained by a transandean migration by an Andean corridor from Argentina, as it was suggested by Casamiquela (1969), or by a southward migration of this species along the Pacific coast from Peru. Both hypotheses should be considered until more evidence that supports one or the other emerges.

ACKNOWLEDGEMENTS

We would like to thank the staff of Museo Nacional de Historia Natural, Chile, for giving us the opportunity to carry out this work. We also want to thank Robert McAfee, Timothy Gaudin, Ana Maria Ribeiro, Leonardo Pérez, Susana Bargo, Rafael Labarca, Graciela Esteban, Castor Cartelle, Sergio Soto and Natalia Villavicencio, all of whom cordially answered some questions and in some cases provided the information required to perform the analyses showed in this work. This study benefited greatly from the constructive review of Robert McAfee that clearly improved this manuscript. Finally, we thank Stephan Püschel for his assistance in the treatment of some images used in the present work.

BIBLIOGRAPHIC REFERENCES

- ALLEN, G.M.
1913 A new *Mylodon*. Memoirs of the Museum of Comparative Zoology at Harvard College 40:319–346.
- BARRIENTOS, G.
1999 Composición isotópica ($\delta^{13}C$) de muestras de restos óseos humanos del sitio Arroyo Seco 2 (Provincia de Buenos Aires): inferencias paleodietarias. Relaciones de la Sociedad Argentina de Antropología XXIV, 81-94.
- BOCHERENS, H., COTTE, M., BONINI, R., SCIAN, D., STRACCIA, P., SOIBELZON, L. and F. J. PREVOSTI
2016 Paleobiology of sabretooth cat *Smilodon populator* in the Pampean Region (Buenos Aires Province, Argentina) around the Last Glacial Maximum: Insights from carbon and nitrogen stable isotopes in bone collagen. Palaeogeography, Palaeoclimatology, Palaeoecology, 449, 463-474.
- BOCHERENS, H., COTTE, M., BONINI, R. A., STRACCIA, P., SCIAN, D., SOIBELZON, L. and F. J. PREVOSTI
2017 Isotopic insight on paleodiet of extinct Pleistocene megafaunal Xenarthrans from Argentina. Gondwana Research, 48, 7-14.
- BURMEISTER, H.
1865 Skin of *Mylodon*. Archive für Anatomie, Physiologie und wissenschaftliche Medicin 1865: 317–334.
- CABRERA, A.
1936 Las especies del género *Glossotherium*. Notas Museo de La Plata, 1: 193–206.
- CARLINI, A. and G.J. SCILLATO-YANÉ
1999 Evolution of Quaternary xenarthrans (Mammalia) of Argentina. Quaternary of South America and Antarctic Peninsula 10: 149–175.
- CARTAJENA, I., LÓPEZ, P., CARABIAS, D., MORALES, C., VARGAS, G. and C. ORTEGA
2013 First evidence of an underwater Final Pleistocene terrestrial extinct faunal bone assemblage from Central Chile (South America): Taxonomic and taphonomic analyses. Quaternary international, 305, 45-55.
- CARTELLE, C. and J.A. FONSECA
1981 Species of the genus *Glossotherium* of Brazil. Anais do II Congresso Latino-Americano de Paleontología 2: 805–818.
- CASAMIQUELA, R.M.
1968 Noticias sobre la presencia de *Glossotherium* (Xenarthra, Mylodontidae) en Chile central. Anales del Museo de Historia Natural 1: 59-75.
- CASAMIQUELA, R.M.
1969 Enumeración crítica de los mamíferos continentales Pleistocenos de Chile. Rehue 2: 143-172. Concepción.
- CASAMIQUELA, R.M.
1976 Los vertebrados fósiles de Tagua-Tagua. I Congreso Geológico Chileno (2-7 de Agosto), Actas 1:C87-C102. Santiago.
- COPE, E.D.
1889 The Edentata of North America. American Naturalist 23: 657–664
- CUVIER, G.
1823 Sur le *Megatherium*. Recherches sur les Ossements Fossiles, 2me Edition, 5:174-192.
- CZERWONOGORA, A., FARINA, R. and E. TONNI
2011 Diet and isotopes of late Pleistocene ground sloths: first results for *Lestodon* and *Glossotherium* (Xenarthra, Tardigrada). Neues Jahrbuch für Geologie und Paläontologie-Abhandlungen 262/3, 257-266
- DARROCH, J.N. and J.E. MOSIMANN
1985 Canonical and principal components of shape. Biometrika 72(2): 241-252.
- DAUDIN, T.J.
2004 Phylogenetic relationships among sloths (Mammalia, Xenarthra, Tardigrada): the craniodental evidence. Zoological Journal of the Linnean Society 140(2): 255-305.
- DE IULIIS, G. and C. CARTELLE
1994 The medial carpal and metacarpal elements of *Eremotherium* and *Megatherium* (Xenarthra: Mammalia). Journal of Vertebrate Paleontology, 13(4), 525-533.
- DELSUC, F., F.M. CTZEFLIS, M.J. STANHOPE and E.J. DOUZERY.
2001 The evolution of armadillos, anteaters and sloths depicted by nuclear and mitochondrial phylogenies: implications for the status of the enigmatic fossil *Eurotamandua*. Proceedings of the Royal Society of London Biological Sciences 268(1476): 1605-1615.

- ESTEBAN, G.
1996 Revisión de los Mylodontinae cuaternarios (Edentata, Tardigrada) de Argentina, Bolivia y Uruguay. Sistemática, Filogenia, Paleobiología, Paleozoogeografía y Paleoecología. Tesis Doctoral, Facultad de Ciencias Naturales, Instituto Miguel Lillo, 235 p.
- FARIÑA, R.A., S.F. VIZCAÍNO and G. DE LULIIS
2013 Megafauna: giant beasts of Pleistocene South America. Indiana University Press.
- FIGINI, A.J., J.E. CARBONARI, G.H. GOMEZ, E.P. TONNI and F. FIDALGO
1987 Radiocarbon date of the bony remains from the La Postrera Formation in the Partido de Loberia, Buenos Aires Province, Argentina. *Actas del Congreso Geológico Argentino* 10: 185–188.
- FLYNN, J.J. and C.C. SWISHER
1995 Cenozoic South American Land-mammal ages: correlation to global geochronologies. *In*: Berggren, W.A., Kent, D.V. y Handerbol, J. *Geochronology, Time scales, and Correlation: Framework for a Historical Geology*. SEPM Special Publication: 317-333.
- FLOWER, W. H.
1873 Note on the carpus of the sloths. *Journal of Anatomy and Physiology, 2nd Series* 7:255-256
- FLOWER, W. H.
1885 An Introduction to the Osteology of the Mammalia, 3rd ed. MacMillan and Co., London, 382 pp.
- GERVAIS, P. and F. AMEGHINO
1880 The fossil mammals of South America. Buenos Aires and Paris: F. Savy.
- GILL, T.
1872 Arrangements of the families of mammals, with analytical tables. *Smithsonian Miscellaneous Collections* 11:1–98.
- HALL, B. K. (ED.).
2008 Fins into limbs: evolution, development, and transformation. University of Chicago Press.
- HARO, J. A., TAUBER, A. A., and J. M. KRAPOVICKAS
2016 The manus of *Mylodon darwini* Owen (Tardigrada, Mylodontidae) and its phylogenetic implications. *Journal of Vertebrate Paleontology*, 36(5), e1188824.
- HILL, R. V.
2006 Comparative anatomy and histology of xenarthran osteoderms. *Journal of Morphology*, 267(12), 1441-1460.
- HUMPHRY, G. M.
1870 The myology of the limbs of the unau, the ai , the two-toed anteater, and the pangolin. *Journal of Anatomy and Physiology, 2nd Series* 4: 17- 78.
- JACKSON, D., MÉNDEZ, C., LÓPEZ, P., JACKSON, D. and R. SEGUEL
2005 Evaluación de un asentamiento arqueológico en el semiárido de Chile: procesos de formación, fauna extinta y componentes culturales. *Intersecciones en Antropología* 6, 139-152.
- JACKSON, D., MÉNDEZ, C., SEGUEL, R., MALDONADO, A. and G. VARGAS
2007 Initial occupation of the Pacific coast of Chile during late Pleistocene times. *Current Anthropology* 48 (5), 725-731.
- JUNGERS, W.L., A.B. FALSETTI and C.E. WALL
1995 Shape, relative size, and size adjustments in morphometrics. *American Journal of Physical Anthropology* 38(S21): 137-161.
- KAHLE D. and H. WICKHAM
2016 Package ‘ggmap’. R package version 2.6.1. <https://cran.r-project.org/web/packages/ggmap/ggmap.pdf>.
- KRAGLIEVICH, L.
1922 Estudios sobre los Mylodontinae: análisis comparado de los valores craneométricos de los milodontinos de Norte y Sud América. *Anales Museo Nacional de Historia Natural de Buenos Aires*, 31: 457–464.
- LABARCA, L.
2015 La meso y megafauna terrestre extinta del Pleistoceno de Chile. *Publicación Ocasional del Museo Nacional de Historia Natural* 63: 412-416.
- LEIDY, J.
1855 A memoir on the extinct sloth tribe of North America. *Smithson Contribution to Knowledge* 7:1–68.
- LÓPEZ MENDOZA, P., CARTAJENA, I., CARABIAS, D., PREVOSTI, F. J., MALDONADO, A. and V. FLORES-AQUEVEQUE
2016 Reconstructing drowned terrestrial landscapes. Isotopic paleoecology of a late Pleistocene extinct faunal assemblage: Site GNL Quintero 1 (GNLQ1) (32° S, Central Chile). *Quaternary International*, In Press, Corrected Proof [Available online 29 September 2016]

- MARKOW, T.A. (Ed.).
2012 Developmental instability: its origins and evolutionary implications: proceedings of the International Conference on Developmental Instability: It's Origins and Evolutionary Implications, Tempe, Arizona, 14–15 June 1993 (Vol. 2). Springer Science & Business Media.
- MARTIN, F. M.
2016 Cueva del Milodón. The hunting grounds of the Patagonian panther. *Quaternary International*. In Press, Corrected Proof.
- MCAFEE, R.K.
2007 Reassessing the Taxonomy and Affinities of the Mylodontinae Sloths, *Glossotherium* and *Paramylodon* (Mammalia: Xenarthra: Tardigrada). Ph.D. Dissertation, Northern Illinois University. DeKalb, IL: 177pp.
- MCAFEE, R.K.
2009 Reassessment of the cranial characters of *Glossotherium* and *Paramylodon* (Mammalia: Xenarthra: Mylodontidae). *Zoological Journal of the Linnean Society* 155: 885–903.
- MCAFEE, R. K.
2016 Description of New Postcranial Elements of *Myiodon darwinii* Owen 1839 (Mammalia: Pilosa: Mylodontinae), and Functional Morphology of the Forelimb. *Ameghiniana*, 53(4), 418-443.
- MCDONALD, H. G.
1987 A systematic review of the Plio-Pleistocene scelidotherine ground sloths (Mammalia: Xenarthra: Mylodontidae). Ph.D. dissertation, University of Toronto, Toronto, Ontario, Canada, 478 pp.
- MCKENNA, M. C. and S. K. BELL
1997 Classification of mammals: above the species level. Columbia University Press. 631 p.
- MÉNDEZ, C., JACKSON, D. and R. SEGUEL
2004 Narrowing the spatial range of megafaunal distributions on the semiarid coast of Chile. *Current Research in the Pleistocene*, 21, 109-111.
- MENEGAUX, A.
1908 Sur le squelette du membre antérieur de *Bradypus torquatus*, III. *Comptes Rendus de l'Academie des Sciences* 637-640.
- MENEGAUX, A.
1909a A propos d'*Hemibradypus mareyi* Anth. = *Bradypus (Scaeopus) torquatus* (III). *Bulletin de la Société Zoologique de France* 34:27-32.
- MENEGAUX, A.
1909b Contribution l'étude des edentes actuels: famille de bradypodidés. *Archives de Zoologie Expérimentale et Generale*, Ve Série, 1:277-344.
- MERRIAM, J. C.
1906 Recent discoveries of Quaternary mammals in Southern California. *Science*, 24(608): 248-250.
- MORENO, P.I., C. VILLAGRÁN, P.A. MARQUET and L.G. MARSHALL
1994 Quaternary paleobiogeography of northern and central Chile. *Revista Chilena de Historia Natural* 67: 487-502.
- NÚÑEZ, L., J. VARELA, R. CASAMIQUELA and C. VILLAGRÁN
1994a Reconstrucción Multidisciplinaria de la Ocupación Prehistórica de Quereo, Centro de Chile. *Latin American Antiquity* 5 (2), 99-118.
- NÚÑEZ, L., J. VARELA, R. CASAMIQUELA, V. SCHIAPPACASSE, H. NIEMEYER and C. VILLAGRÁN
1994b Cuenca de Tagua Tagua en Chile: El ambiente del Pleistoceno Superior y ocupaciones humanas. *Revista Chilena de Historia Natural* 67, 503-519
- OWEN, R.
1840 Zoology of the voyage of the Beagle. Part 1. Fossil Mammalia, 57–106. OWEN, R.
- OWEN, R.
1842 Description of the skeleton of and extinct gigantic sloth, *Myiodon robustus* Owen, with observations on the osteology, natural affinities, and probable habits of the megatherioid quadrupeds in general. London: R. and J. Taylor.
- OWEN, R.
1858 On the *Megatherium (Megatherium americanum)*, Cuvier and Blumenbach). Part IV. Bones of the anterior extremities. *Philosophical Transactions of the Royal Society of London* 148:261-278
- PÉREZ L.M., G.J. SCILLATO-YANÉ and S.F. VIZCAÍNO
2000 Estudio morfofuncional del aparato hioideo de *Glyptodon cf. clavipes* Owen (Cingulata: Glyptodontidae). *Ameghiniana* 37: 293–299.

- PÉREZ, L.M., N. TOLEDO, G. DE IULIIS, M.S. BARGO and S.F. VIZCAÍNO
2010 Morphology and function of the hyoid apparatus of fossil xenarthrans (Mammalia). *Journal of morphology* 271(9): 1119-1133.
- PITANA, V.G., G.I. ESTEBAN, A.M. RIBEIRO and C. CARTELLE
2013 Cranial and dental studies of *Glossotherium robustum* (Owen, 1842) (Xenarthra: Pilosa: Mylodontidae) from the Pleistocene of southern Brazil. *Alcheringa: An Australasian Journal of Palaeontology* 37(2): 147-162.
- PUJOS, F. and R. SALAS
2004 A systematic reassessment and paleogeographic review of fossil Xenarthra from Peru. *Bulletin de l'Institut Français d'Études Andines* 33 (2): 331-377.
- POCHE, F.
1908 Über die Anatomie und die systematische Stellung von *Bradypus torquatus* (IIL) . *Zoologischer Anzeiger* 33:567-580.
- POCHE, F.
1911 Neue Untersuchungen über die Anatomie und die systematische Stellung von *Scaeopus torquatus*, nebst Bemerkungen über die morphologische Bedeutung des basalen Gliedes des Radius I des Saugetierchiridiums. *Archiv für Naturgeschichte* 77: 33-49.
- PRADO, J. L., MARTÍNEZ-MAZA, C., and M. T. ALBERDI
2015 Megafauna extinction in South America: A new chronology for the Argentine Pampas. *Palaeogeography, Palaeoclimatology, Palaeoecology*, 425, 41-49.
- PREVOSTI, F. J. and F. M. MARTIN
2013 Paleoeology of the mammalian predator guild of Southern Patagonia during the latest Pleistocene: ecomorphology, stable isotopes, and taphonomy. *Quaternary International*, 305, 74-84.
- R CORE TEAM
2014 R: A language and environment for statistical computing. R Foundation for Statistical Computing, Vienna, Austria. URL <http://www.R-project.org/>.
- SÁNCHEZ, G.
2013 Discriminer: Tools of the Trade for Discriminant Analysis. R package version 0.1-29. <http://CRAN.R-project.org/package=Discriminer>
- SEGUEL, R., D.G. JACKSON, C.A. MÉNDEZ and P. LÓPEZ
2010 Extinct fauna, palimpsest and scavenging in the semiarid North Coast of Chile. *Current Research in the Pleistocene*, 27, 28-31.
- SINCLAIR, W. J.
1910 Dermal bones of *Paramylodon* from the asphaltum deposits of Rancho La Brea, near Los Angeles, California. *Proceedings of the American Philosophical Society*, 49(195), 191-195.
- SPILLMANN, F.
1931 Ecuador mammals in the time of change. Erster Teil. Quito: Universidad Central.
- STEELE, J. and G. POLITIS
2009 AMS 14C dating of early human occupation of southern South America. *Journal of archaeological science*, 36(2), 419-429.
- STOCK, C.
1925 Cenozoic Gravigrade Edentates of Western North America: With Special Reference to the Pleistocene Megalonychinae and Mylodontidae of Rancho La Brea (No. 331). Carnegie Institution of Washington.
- STUIVER, M. AND P. J REIMER
1986–2014 Calib 7.01. – Calibration Radiocarbon Program.
- SUÁREZ, M. AND C. EMPARAN
1997 Hoja Curacautín, Regiones de la Araucanía y del Biobío. Servicio Nacional de Geología y Minería, Carta Geológica de Chile, No. 71, 105 p., 1 mapa 1:250.000.
- SWOFFORD, D.L.
2003 PAUP*. Phylogenetic Analysis Using Parsimony (*and Other Methods). Version 4. Sinauer Associates, Sunderland, Massachusetts.
- TAMBUSSO, P. S., MCDONALD, H. G. and R.A FARIÑA
2015 Description of the stylohyal bone of a giant sloth (*Lestodon armatus*). *Palaeontologia Electronica*, 18(1), 1-10
- THIELE, R., A. LAHSEN, H. MORENO, J. VARELA, M. VERGARA and F. MUNIZAGA
1987 Estudio Geológico Regional a Escala 1: 100.000 de la Hoya superior y curso medio del río Biobío. ENDESA-Departamento de Geología y Geofísica, Universidad de Chile. Informe Inédito.

WOODWARD, A.S., and F.P. MORENO

1899 On a Portion of Mammalian Skin, named *Neomylodon listai*, from a Cavern near Consuelo Cove, Last Hope Inlet, Patagonia. In Proceedings of the Zoological Society of London (Vol. 67, No. 1, pp. 144-156). Blackwell Publishing Ltd.

VAN BUUREN, S., K. GROOTHUIS-OUDSHOORN, A. ROBITZSCH, G. VINK, L. DOOVE and S. JOLANI 2015 Package 'mice'. R package version 2.25. <https://cran.r-project.org/web/packages/mice/mice.pdf>.

VARELA, L. and R. A. FARIÑA

2016 Co-occurrence of mylodontid sloths and insights on their potential distributions during the late Pleistocene. Quaternary Research, 85(1), 66-74.

VILLAVICENCIO, N. A.

2016 Late Quaternary Megafaunal Extinctions in South America: Chronology, Environmental Changes and Human Impacts at Regional Scales. PhD Thesis, University of California, Berkeley.

WALKER, M., *et aliter*

2009 Formal definition and dating of the GSSP (Global Stratotype Section and Point) for the base of the Holocene using the Greenland NGRIP ice core, and selected auxiliary records. Journal of Quaternary Science, 24(1), 3-17.